

The Journal of Physiology

<http://jp.msubmit.net>

JP-RP-2016-273735XR1

Title: Low pHo boosts burst firing and catecholamine release by blocking TASK-1 and BK channels while preserving Cav1 channels in mouse chromaffin cells

Authors: Laura Guarina
David Vandael
Valentina Carabelli
Emilio Carbone

Author Conflict: No competing interests declared

Author Contribution: Laura Guarina: Conception and design; Collection and assembly of data; Data analysis and interpretation; Manuscript Writing; Final approval of manuscript (required) David Vandael: Conception and design; Collection and assembly of data; Final approval of manuscript (required) Valentina Carabelli: Collection and assembly of data; Data analysis and interpretation; Manuscript Writing; Final approval of manuscript (required) Emilio Carbone: Conception and design; Financial Support; Data analysis and interpretation; Manuscript Writing; Final approval of manuscript (required)

Running Title: Low pHo-induced burst firing in chromaffin cells

Dual Publication: No

Funding: Ministero dell'Istruzione, dell'Università e della Ricerca (Ministry of Education, Research and Universities): Emilio Carbone, PRIN 2010/2011project

Disclaimer: This is a confidential document.

2010JFYFFY2; Telethon Foundation: Emilio Carbone, grant # GGP15110; University of
Torino: Emilio Carbone, local grants

Low pHo boosts burst firing and catecholamine release by blocking TASK-1 and BK channels while preserving Cav1 channels in mouse chromaffin cells

Laura Guarina¹, David H.F. Vandael^{†1}, Valentina Carabelli¹, Emilio Carbone^{1§}

¹*Department of Drug Science, Laboratory of Cellular and Molecular Neuroscience, N.I.S. Centre, CNISM Unit, 10125 Torino, Italy*

Running title: Low pHo-induced burst firing in chromaffin cells

Keywords: BK channels, TASK-1 channels, L-type Cav1 channels

§ *Corresponding author:* Emilio Carbone
Department of Drug Science
Corso Raffaello 30
10125 - Torino, Italy
e-mail: emilio.carbone@unito.it

† *Present address:* Institute of Science and Technology Austria
Am Campus 1
A – 3400 Klosterneuburg, Austria
e-mail: david.vandael@ist.ac.at

Key points

- Mouse chromaffin cells (MCCs) generate spontaneous burst-firing that causes massive increases of Ca^{2+} -dependent catecholamine release, and is thus a key mechanism to regulate MCCs functions.
- With the purpose of uncovering a physiological role for burst-firing, we studied the effects of acidosis on MCCs activity.
- We found that lowering extracellular pH (pH_o) from 7.4 to 6.6 induces 10-15 mV cell depolarizations that generate bursts of ~330 ms at 1-2 Hz and a 7.4-fold increase of catecholamine-cumulative release.
- Burst-firing originates from the inhibition of the pH-sensitive TASK1-channels and 60% reduction of BK-channel conductance at pH_o 6.6.
- Blockers of the two channels (A1899 and paxilline) mimic the effects of pH_o 6.6 that are reverted by the Cav1 channel blocker nifedipine.
- MCCs act as pH-sensors. In low pH_o they depolarize, undergo burst-firing and increase CA-secretion, generating an effective physiological response that may compensate acute acidosis and hyperkalemia generated during heavy exercise and muscle fatigue.

Abstract

Mouse chromaffin cells (MCCs) generate action potential (AP) firing that regulates the Ca^{2+} -dependent release of catecholamines (CAs). Recent findings indicate that MCCs possess a variety of spontaneous firing modes that span from the common “tonic-irregular” to the less frequent “burst” firing. This latter is evident in a small fraction of MCCs but occurs regularly when Nav1.3/1.7 channels are made less available or when the Slo1 β 2-subunit responsible for BK channel inactivation is deleted. Burst firing causes massive increases of Ca^{2+} -entry and potentiates CA release ~3.5-fold and, thus, may be a key mechanism to regulate MCC function. With the purpose of uncovering a physiological role for burst firing in CCs, we studied the effects of acidosis on MCCs activity.

We found that lowering extracellular pH (pH_o) from 7.4 to 7.0 and 6.6 induces 10-15 mV cell depolarizations that generate repeated bursts. Bursts at pH_o 6.6 lasted ~330 ms, occurred at 1-2 Hz and caused ~7-fold increase of CA cumulative release. Burst firing originates from the inhibition of the pH-sensitive TASK-1/TASK-3 channels and from a 40% BK channel conductance reduction at pH_o 7.0. The same pH_o had little or no effect on Nav, Cav, Kv and SK channels that support AP firing in MCCs. Burst firing of pH_o 6.6 could be mimicked by mixtures of the TASK-1 blocker A1899 (300nM) and BK blocker paxilline (300nM) and could be prevented by blocking L-type channels by adding 3 μM nifedipine. Mixtures of the two blockers raised cumulative CA-secretion even more than low- pH_o (~12-fold), showing that the action of protons on vesicle release is mainly due to the ionic conductance changes that increase Ca^{2+} -entry during bursts.

Our data furnish direct evidence that MCCs respond to low- pH_o with sustained depolarization, burst firing and enhanced CA-secretion, thus mimicking the physiological response of CCs to acute acidosis and hyperkalemia generated during heavy exercise and muscle fatigue.

Abbreviations: AHP after-hyperpolarization; AP, action potential; CA, catecholamine; CC, chromaffin cells; CFE, carbon fibre electrode; DHP, dihydropyridine; ISI, interspike interval; BCC, bovine chromaffin cell; MCC, mouse chromaffin cell; RCC, rat chromaffin cell.

Introduction

Chromaffin cells (CCs) of the adrenal medulla undergo spontaneous firing at rest and respond to sustained depolarization with trains of action potentials (APs) that rapidly adapt their firing to higher frequencies (Nassar-Gentina *et al.*, 1988; Martinez-Espinosa *et al.*, 2014; Vandael *et al.*, 2015a). The molecular components of this phenomenon have been identified in mouse CCs (MCCs). AP firing is generated by fast inactivating TTX-sensitive Nav1.3/Nav1.7 sodium channels that sustain the AP upstroke, while slowly inactivating L-type Ca²⁺ channels (Cav1) contribute to the slow depolarization phase during prolonged interspike intervals (Vandael *et al.*, 2015b). AP repolarization is ensured by voltage-gated K⁺ channels and by the differential coupling of voltage-gated Cav channels to BK and SK channels (Marcantoni *et al.*, 2010; Vandael *et al.*, 2010; Vandael *et al.*, 2012). Opening of BK and SK channels set the shape and frequency of APs, as well as their mode of adaptation during sustained depolarizations (Vandael *et al.*, 2015a).

Recently, we reported that a reduction of Nav1.3/Nav1.7 channel availability due to slow inactivation during sustained depolarizations or block by TTX cause a sudden switch from tonic to burst firing with consequent increase of Ca²⁺ influx during the burst and marked rise of catecholamine (CA) release in MCCs (Vandael *et al.*, 2015b). Burst firing occurs also upon deletion of the Slo1β2 subunits responsible for the fast inactivation of voltage- and Ca²⁺-dependent BK channels (Martinez-Espinosa *et al.*, 2014), and is also evident in a small fraction (10-15%) of resting control MCCs (Martinez-Espinosa *et al.*, 2014; Vandael *et al.*, 2015b). Thus, chromaffin cells possess spontaneous “neuron-like” firing modes that boost the non-neurogenic Ca²⁺-dependent release of CAs when specific membrane conductances are modulated. This endogenous burst behavior may represent a simple mechanism by which CCs and other neuroendocrine cells potentiate Ca²⁺ entry and hormone release during specific physiological stimuli. Given that bursting pacemaker activity and other patterns of similar electrical activity may arise from a number of distinct ionic conductances (Marder & Taylor, 2011), it is of extreme interest to identify the existence of other ionic mechanism able to induce burst firing in MCCs, besides a reduction of Nav channel availability and deletion of Slo1β2 subunits (Lingle, 2015). Regarding this, it would be of key importance to understand whether burst firing in MCCs arises also during physiological stimuli causing robust membrane depolarization such as blood acidosis, hyperkalemia, elevation of histamine and increased levels of muscarine induced by splanchnic nerve stimulation (Neely & Lingle, 1992; Inoue *et al.*, 1998; Wallace *et al.*, 2002; Inoue *et al.*, 2008; Mahapatra *et al.*, 2011).

Here we show that isolated MCCs respond to low extracellular pH (pH_o) with sustained depolarization, burst firing and enhanced CAs exocytosis. Lowering pH_o from 7.4 to 7.0 and 6.6 induces robust depolarizations that switch spontaneous tonic firing into regular bursts. Burst firing at low pH_o is due to the inhibition of pH-sensitive TASK-1 and TASK-3 “leak” channels (Cotten, 2013; Bayliss *et al.*, 2015) and Ca²⁺-dependent BK channels (Prakriya & Lingle, 1999). The other channels responsible of AP firing in MCCs (Kv, Nav, Cav and SK) are weakly or not affected by

low pH_o. Mixtures of the TASK-1 channel blocker A1899 (Streit *et al.*, 2011) and paxilline (a blocker of BK channels) can nicely reproduce the effects of pH_o 6.6. On the contrary, nifedipine can either revert regular bursts into tonic firing or block the firing, suggesting a key role of Cav1 channels in the generation of the plateau potential of bursts in MCCs (Vandael *et al.*, 2015b).

Using amperometry, we also show that burst firing induced by acidic pH_o or mixtures of A1899 and paxilline causes a marked increase of CA cumulative release, mainly due to an elevated rate of vesicle release. The similar action of low pH_o and mixtures of TASK-1 and BK channel blockers suggests that the acute action of protons on CA release in MCCs is mainly due to ionic conductance changes that boost Ca²⁺ entry during bursts rather than to specific effects of protons on the secretory apparatus (Jankowski *et al.*, 1993).

Our data furnish new evidence that burst firings in CCs is likely to be an effective mechanism that regulates the feedback response of adrenal glands to acute blood acidosis and hyperkalemia by increasing circulating CA (Cryer, 1980; Medbo & Sejersted, 1990).

Methods

Ethical approval - Ethical approval was obtained for all experimental protocols from the University of Torino Animal Care and Use Committee, Torino, Italy. All experiments were conducted in accordance with the National Guide for the Care and Use of Laboratory Animals adopted by the Italian Ministry of Health. Every effort was made to minimize animal suffering and the number of animals used. For removal of tissues, animals were deeply anaesthetized with CO₂ inhalation and rapidly killed by cervical dislocation.

Cell culture - Chromaffin cells were obtained from male C57BL/6J mice (Harlan, Correzzano, Italy) of 2 months. Under sterile conditions the abdomen was opened, the adrenal glands were isolated, and transferred to an ice cold Ca²⁺ and Mg²⁺ free Locke's buffer containing (in mM) 154 NaCl, 3.6 KCl, 5.6 NaHCO₃, 5.6 glucose and 10 HEPES, pH 7.4 (Marcantoni *et al.*, 2009; Vandael *et al.*, 2012). Under a dissecting microscope the adrenal glands were decapsulated and subsequently subjected to an enzymatic dissociation with 20-25 units/ml papain (Worthington Biochemical Corporation, Segrate, Italy) dissolved in DMEM (GIBCO, Invitrogen Life Technologies, Monza, Italy) supplemented with 1.5 mM of L-cysteine, 1 mM of CaCl₂ and 0.5 mM of EDTA (Sigma Aldrich, Munich, Germany) for 25 -30 minutes at 37°C in a water saturated atmosphere with 5% CO₂. Afterwards, two washing steps were performed with DMEM supplemented with 1mM CaCl₂ and 10 mg/ml of BSA (Sigma Aldrich). Adrenal medulla's were re-suspended in DMEM containing 1% pen/strep and 15% fetal bovine serum (both from Sigma Aldrich) and were mechanically dissociated with a fire polished Pasteur pipette. A drop (100 µL) of this concentrated cell suspension was plated on poly-ornithine (1mg/ml) and laminin (5 µg/ml) coated petri- dishes and subsequently

(30 minutes later) 1.9 ml of DMEM containing 1% pen/strep and 15% fetal bovine serum (all from Sigma Aldrich) was added. The primary chromaffin cell cultures were kept in an incubator at 37°C at water saturated atmosphere with 5% CO₂. Measurements were performed on cultured MCCs two to five days after plating.

Action potentials and ion currents recordings - Macroscopic whole-cell currents and APs were recorded in perforated-patch conditions using a multiclamp 700-B amplifier and pClamp 10.0 software (Molecular Devices, Sunnyvale, CA, USA) (Marcantoni *et al.*, 2010; Vandael *et al.*, 2012). Traces were sampled at 10 KHz using a digidata 1440 A acquisition interface (Molecular Devices, Sunnyvale, CA, USA) and filtered using a low-pass Bessel filter set at 1-2 KHz. Borosilicate glass pipettes (Kimble Chase life science, Vineland, NJ, USA) with a resistance of 2-3 MΩ were dipped in an eppendorf tube containing intracellular solution before being back filled with the same solution containing 500µg/ml of amphotericin B (Sigma Aldrich, Munich, Germany), dissolved in DMSO (Sigma Aldrich, Munich, Germany) (Cesetti *et al.*, 2003). Recordings were initiated after amphotericin B lowered the access resistance below 15 MΩ (5-10 min). Series resistance was compensated by 60-80% and monitored throughout the experiment. Fast capacitive transients during step-wise depolarisations (in voltage-clamp mode) were minimized online by the use of the patch clamp analogue compensation. Uncompensated capacitive currents were further reduced by subtracting the averaged currents in response to P/4 hyperpolarising pulses.

The normalized voltage-dependent conductance of Nav channels (g_{Na}), was calculated with the equation: $g_{Na} = I_{Na\text{peak}} / (V - V_{\text{rev}})$, with V_{rev} equal to the reversal potential for Na⁺, and fitted with a Boltzmann function with variable $V_{1/2}$ (in mV) and k slope (in mV). The same was done for g_{Ca} and g_{BK} .

Amperometric current recordings during low pHo-induced burst firing – Simultaneous detection of amperometric currents associated with CA release and AP recordings was performed using a HEKA EPC-10 double amplifier. For amperometry, we used standard carbon fiber microelectrodes (CFEs) of 5 µm tip diameter polarized at +800 mV (ALA Scientific Instruments Inc.; Westbury, NY, USA) (Carabelli *et al.*, 2007; Marcantoni *et al.*, 2009; Vandael *et al.*, 2015b). For the current-clamp AP recordings, we used glass pipettes and perforated patch conditions as described above. The CFE was first placed sidewise adjacent to the cell, taking care to leave part of the cell surface accessible to the glass pipette for recording APs. The glass pipette was positioned opposite to the CFE on the free available side of the cell. While recording amperometric signals, the spontaneous APs that appeared as “irregular tonic” firing at pHo 7.4 were converted to “burst” firing by either lowering pHo to 6.6 or adding mixtures of A1899 (300 nM) and paxilline (300 nM) to the external solution. Amperometric currents were sampled at 4 kHz and low-pass filtered at 1 kHz. Data were analysed by IGOR macros Quanta_analysis (WaveMetrics, Lake Oswego, OR, USA) as described elsewhere (Carabelli *et al.*, 2007). The analysis of individual exocytotic events was done by measuring the following parameters: maximum oxidation current (I_{max}), spike width

at half height ($t_{1/2}$), total charge of the spike (Q), cubic root of Q ($Q^{1/3}$) and time to reach the spike (t_p). All experiments were performed at room temperature.

Solutions - Intracellular solution for current-clamp and Na^+ and K^+ current measurements in voltage clamp or AP-clamp mode was composed of (in mM) 135 KAsp, 8 NaCl, 2 MgCl_2 , 5 EGTA, 20 HEPES, pH 7.4 (with KOH; Sigma Aldrich). For Ca^{2+} current recordings the intracellular solution contained (in mM) 135 Cs-MeSO₃, 8 NaCl, 2 MgCl_2 , 5 EGTA and 20 HEPES, pHo 7,4 (with CsOH; Sigma Aldrich). The extracellular solution used for current-clamp measurements is a physiological Tyrode's solution containing in mM: 130 NaCl, 4 KCl, 2 CaCl_2 , 2 MgCl_2 , 10 glucose and 10 HEPES; pHo 7.4 (with NaOH; Sigma Aldrich). The same solution was used to measure K^+ currents. K_v currents were obtained by adding 500 μM Cd^{2+} to the external solution while Ca^{2+} -activated BK currents were estimated by subtracting K_v from the total K^+ currents. As previously noted (Vandael *et al.*, 2015b), residual Cd^{2+} -insensitive voltage-dependent BK currents contribute little (< 5%) to the total BK currents at +20 to +30 mV (Berkefeld & Fakler, 2013). Thus, isolation of BK currents using 500 μM Cd^{2+} appears a reliable protocol. The extracellular solution used for Na^+ current measurements was composed of (in mM): 104 NaCl, 30 TEACl, 4 KCl, 2 CaCl_2 , 2 MgCl_2 , 10 glucose and 10 HEPES, pHo 7,4 (with NaOH). The extracellular solution used for Ca^{2+} current measurements in voltage-clamp configuration contained (in mM): 135 TEACl, 2 CaCl_2 , 2 MgCl_2 , 10 glucose and 10 HEPES, pHo 7.4 (with TEA-OH; Sigma Aldrich). The extracellular pHo of the bath solutions was adjusted individually adding HCl to reach the following values: 7.2, 7.0, 6.8 and 6.6. Addition of HCl to obtain pHo 6.6 increased the osmolality of the solution by < 2%. This small osmolality change was found of no effect on cell excitability.

The liquid junction potential (LJP) of the solutions was calculated using the JPCalcWin program available from Axon Instrument (Clampex, version 10.5) that is derived from the original software package of P.H. Barry (Barry, 1994). For the solutions used, the uncompensated LJP was +12.6 mV for the current-clamp and K^+ current, +13.5 mV for the Na^+ current and +16.6 mV for the Ca^{2+} current measurements at 22°C. These values should be further corrected for the Donnan equilibrium potential that generates at the perforated patch (V_{pf}) (Horn & Marty, 1988). V_{pf} was estimated in the order of 2.6 mV for the current-clamp, K^+ and Na^+ currents and 3.4 mV for the Ca^{2+} currents and was subtracted from the LJP. Following the subtraction, the uncompensated LJPs were +10, +10,9 and +13.2 mV for the three cases indicated above. Since addition of the drug tested has nearly no effect on the LJP and lowering of pHo with HCl causes voltage changes of ~1 mV, the membrane potentials of our current- and voltage-clamp recordings were not corrected for the different LJPs.

Testing the effects of low pHo required usually 1 min to reach steady-state conditions. Wash out was also rapid when testing the effects of pHo on Nav, Cav, Kv and SK channels given the small effects observed. The recovery was significantly slower (3 to 6 min) when washing out the effects

of pHo on BK currents, most likely because the inhibitory effects on these channels are mainly due to a lowering of the intracellular pH (see Discussion and Kume *et al.*, 1990).

TASK-1 and TASK-3 blockers (PK-THPP and A1899) (Streit *et al.*, 2011; Coburn *et al.*, 2012) were purchased from Aberjona Laboratories (Woburn, MA), dissolved in DMSO and stored at -20°C. Nifedipine and BayK8644 were obtained from Sigma Aldrich. The two dihydropyridines (DHPs) were dissolved, stored and used as previously described (Carabelli *et al.*, 2001).

Analysis - Data are given as mean \pm SEM for n number of cells. Statistical significance was estimated using either paired/unpaired Student t-tests or one-way ANOVA followed by a Bonferroni *post hoc* test in case of two or multiple groups of measurements had to be compared. Data were found statistically significant when $P \leq 0.05$. Statistical analysis was performed with SPSS software (version 20.0, IBM). Off-line data analysis was performed with pClamp and Origin (OriginLab Corporation, Northampton, MA, USA) software.

Results

Low extracellular pH induces cell depolarization and burst firing in MCCs

Our first goal was to assess how lowering pHo from 7.4 to 6.6 altered both the resting potential and the spontaneous firing modes of MCCs in current-clamp conditions with no current injection (Fig. 1a). Slight changes in pHo (from 7.4 to 7.0) were sufficient to evoke tonic firing of increased frequency (from 0.43 ± 0.07 Hz to 1.36 ± 0.33 Hz; $n = 9$, $P < 0.01$, paired Student's t test) (Fig. 1a, b), associated with ~ 7 mV cell depolarization of resting potential (V_{rest}) (Fig. 1c). Lower pHo caused increased cell depolarization and resting firing frequency. Mean frequency was 2.05 Hz at pHo 6.8 and 2.52 Hz at pHo 6.6 (Fig. 1b). The pH-dependence of V_{rest} followed a dose-response curve with -35.1 mV at pHo 6.6, -51.0 mV at pHo 7.6 and $IC_{50} = 7.2$ (Fig. 1c). Thus, a Δ pH excursion from 7.6 to 6.6 was sufficient to depolarize the MCCs by about 16 mV (Fig. 1c) and cause increased rate of firing from 0.15 Hz to 2.5 Hz (Fig. 1b). The effects of lowering pHo were always tested after recording spontaneous MCCs activity at pHo 7.4 for 60 to 90 s to ensure stable cell activity. Resting depolarization and increased firing frequency induced by low pHo required usually 20 to 40 s to reach steady-state values and were fully reversible after 2-3 min of continuous washing (Fig. 1d). On average, MCCs firing activity was stable for 5 to 6 min (occasionally for 10 min), which was a time lapse sufficient for testing the effects of low pHo. Cells with fluctuating resting potential ($\Delta V_{rest} = \pm 8$ mV), with APs below 0 mV or with AP firing often interrupted by silent periods longer than 20 s were disregarded from the analysis.

Lowering pHo did not cause only a simple increase of firing frequency. Starting from pHo 7.0 we observed that spontaneous firing of MCCs switched from "irregular tonic" to "burst" firing as already reported during sustained depolarization or partial block of Nav1.3/Nav1.7 channels in MCCs

(Vandael *et al.*, 2015a; Vandael *et al.*, 2015b). The probability of observing burst firing increased with lowering pH_o to reach almost permanent burst-like firing conditions at pH_o 6.6 (Fig. 1a). The switch from tonic to burst firing was particularly evident in the distribution of the interspike interval (ISI) duration. At pH_o 7.4 and 7.2 the distribution had a broad range of ISI values (from 0.03 to 3 s) reflecting the irregular tonic firing of the cells (Fig. 2). At pH_o < 7.0 two separate Gaussian distributions with distinct peaks became evident. The 1st peak (brief durations) represents the ISI between two consecutive spikes within a burst (intra-burst interval), whereas the 2nd peak at longer times represents the ISI between consecutive bursts (inter-burst interval) (Vandael *et al.*, 2015b). The mean intra-burst interval was 32, 17, and 9 ms at pH_o 7.0, 6.8 and 6.6, whereas the Gaussian distribution of the inter-burst intervals peaked at 394, 360 and 331 ms at pH_o 7.0, 6.8 and 6.6, respectively. When we plotted each ISI (ISI_i) against its successive ISI (ISI_{i+1}), we could distinguish a clear difference between pH_o 7.4 and pH_o < 7.0 (bottom panels in Fig. 2). In these ISI_i/ISI_{i+1} graphs with the ISI_i plotted along the x-axis and the ISI_{i+1} plotted along the y-axis, the irregular “tonic” firing patterns gave rise to a random distribution of events, whereas a moderate burst firing gave rise to “L-shaped” distributions. This is clearly visible at pH_o 7.0 and pH_o 6.8, where the “L-shaped” distribution is best evident. At pH_o 6.6 burst firing was more sustained leading to a shorter inter-burst interval that causes a less well-resolved “L-shaped” distribution.

Block of TASK-1 and TASK-3 leak channels causes cell depolarization and burst firing in MCCs

Recent work suggests that chromaffin cell depolarization induced by low pH_o is mainly associated with the block of two-pore TASK-1 and TASK-3 K⁺ channels family (Inoue *et al.*, 2008). Following this, we tested whether TASK-1 and TASK-3 blockers (PK-THPP and A1899) induce MCCs sustained depolarization and generate burst firing similar to low pH_o. PK-THPP is reported to block TASK-3 channels with high affinity (IC₅₀ = 35 ± 5 nM) (Coburn *et al.*, 2012) and TASK-1 with a nearly 10-fold lower affinity (IC₅₀ = 300 ± 20 nM), while A1899 is reported more selective for TASK-1 channels (IC₅₀ = 35 ± 3.8 nM) and less selective toward TASK-3 (IC₅₀ = 318 ± 30 nM) (Streit *et al.*, 2011). Given this, we tested the blocking activity of both compounds at 300 nM, in order to get ~50% block of the channel with lower affinity and almost complete block of the channel with higher affinity (Fig. 3). Specifically, in the case of 300 nM A1899 we expected 50% block of TASK-3 and 100% block of TASK-1 and the opposite with PK-THPP. We found that 300 nM A1899 caused a mean depolarization of 4.5 mV (from -48.2 n = 11 to -43.7 mV; n = 15, P < 0.001, one-way ANOVA; Fig. 3c) and a net AP frequency increase from 0.83 to 1.74 Hz (P < 0.001, one-way ANOVA; Fig. 3c) and brief periods of burst firing activity (see grey insets in Fig. 3a). PK-THPP produced remarkably lower depolarizations and less moderate increase of AP firing that were not statistically significant (P > 0.05, one-way ANOVA). Prolonged applications of A1899 (300 nM) and addition of PK-THPP (300 nM) that lasted altogether 2-3 min caused only slight increased depolarizations (-42.6 mV; n = 7) and firing frequency (1.89 Hz; n = 7), not statistically different from the effects of

A1899 alone ($P > 0.05$, one-way ANOVA; Fig. 3d). The reversibility of A1899 action was not tested systematically since the drug was never washed during all the experiments (see below). In few cells, we found a significant recovery that could not be complete due to the deteriorated conditions of the cell at the end of the experiment.

Accurate analysis of ISI distribution showed that 300 nM A1899 or mixtures of 300 nM A1899 + 300 nM PK-THPP caused burst firings that were similar to pH_o 7.0 but significantly different from pH_o 6.6 (see below). In conclusion, block of TASK-1/TASK-3 channels by either A1899, PK-THPP or both does not account for the marked cell depolarization and sustained burst firing induced by lowering pH_o below 7.4. We therefore hypothesized that low pH_o could induce marked resting depolarizations and sustained burst firing by inhibiting also other K^+ channels (BK, SK and Kv), while preserving or mildly affecting Cav or Nav channels that sustain the inward currents underlying the bursts (Marcantoni *et al.*, 2010; Vandael *et al.*, 2015b). We, thus, studied the effects of pH_o on the ionic conductances sustaining the spontaneous AP firing of MCCs with the idea of identifying the most sensitive K^+ channel whose reduced permeability or altered voltage- and Ca^{2+} -dependence activation could favour membrane depolarization and burst firing modes.

Nav, Cav and SK currents are little or not affected by lowering pH_o

We started by testing the effects of low pH_o on the two major ionic components controlling cell depolarization: Nav and Cav currents. We also decided to limit the pH_o test to 7.0, which is within the physiological pH range and the minimal ΔpH able to induce burst firing. As shown in Fig. 4a, pH_o 7.0 caused almost no change in the amplitude and time course of inward Nav currents activated from -40 to +60 mV. The time difference to reach 90% and 10% of the peak amplitude ($t_{90\%-10\%}$), was taken as an estimate of channel activation and appeared nearly identical between -20 and 0 mV (left inset in panel **a**). The same was true for the time constant of inactivation (τ_{inact}) (right inset in panel **a**), whose values correspond to the τ_{inact} values of Nav1.3 channels (Catterall *et al.*, 2005). Mean peak Nav currents at 0 mV were also not significantly different: -1.89 ± 0.22 nA and -1.96 ± 0.19 nA at pH_o 7.4 and 7.0, respectively (inset in panel **b**). The voltage-dependence of normalized I/V and channel conductance curves at pH_o 7.0 was nearly identical to pH_o 7.4 (mean $V_{1/2} = -17.6$ mV at pH_o 7.4 and $V_{1/2} = -16.6$ mV at pH_o 7.0) (Fig. 4b, c).

Minimal gating changes occurred also on voltage-gated Cav channels at pH_o 7.0. Cav currents elicited during pulses of 30 ms from -40 to +60 mV had nearly the same activation time course, while the amplitude was slightly smaller during pulses < 0 mV (Fig. 5a), but equal or larger at positive potentials (not significantly different at all voltages). Mean peak amplitude at 0 mV was: -101.6 ± 24.0 pA and -114.6 ± 21.8 pA at pH_o 7.4 and 7.0, respectively (inset in panel **b**). At pH_o 7.0, the voltage-dependence of normalized I/V and channel conductance curves were shifted by ~ 4 mV to the right, as expected from the Ca^{2+} -induced surface charge screening of high-threshold

Ca²⁺ channel activation described in other cells (Zhou & Jones, 1996) (Fig. 5b, c). The shift increased proportionally to the pHo value: at pHo 7.2, it was ~2 mV and, at pHo 6.8 it was ~6 mV.

Given that burst firing is sustained mainly by slowly inactivating Cav1 channels that carry sufficient inward current during plateau potentials of 300 to 400 ms to -20 mV (Vandael *et al.*, 2015b) we also tested whether the total and L-type (nifedipine-sensitive) Ca²⁺ currents had altered kinetics during step depolarization of 300 ms at -20 and -10 mV. Inward Ca²⁺ currents had only a slight decrease (10-15%; not significant) at pHo 7.0, as expected by the right shift of their voltage-dependent activation, but had nearly the same time course of inactivation of control currents. This was evident by comparing the normalized traces of pHo 7.4 and 7.0 at -10 and -20 mV. As shown in Fig. 5d, total and L-type current traces (estimated after subtraction for nifedipine-insensitive currents) at pHo 7.4 and 7.0 are nearly undistinguishable at both potentials (black and red traces). Double-exponential fits of the averaged normalized traces at control (continuous yellow curves in Fig. 5d) indicate the presence of a fast and slow inactivating component with similar time constants and baseline at both pHo. Single exponential fits of L-type currents had also similar amplitude, time constant and baseline. The amplitude and time constants of the fast (A_f , τ_f) and slow component (A_s , τ_s) and baseline values (C) of the curve fit at pHo 7.4 and 6.6 are given in figure legend 5d. Similar data were obtained in 5 other MCCs.

Low pHo reduces BK channel conductance and has little effect on Kv and SK currents

In contrast to SK channels and regardless of the little effects of pHo on Cav currents, the Ca²⁺ and V-dependent BK channel currents were markedly attenuated when lowering pHo (Fig. 6). To test the action of low pHo, we first determined the Ca²⁺-dependence of BK channel activation by measuring the BK currents activated by 100 ms pre-loading steps of variable voltage (from -60 to +120 mV by steps of 20 mV) to inject variable quantities of Ca²⁺ ions. BK currents were measured at +120 mV to induce maximal BK channel activation (Gavello *et al.*, 2015). We first applied pHo 7.4 and then pHo 7.0 (Fig. 6a). Addition of Cd²⁺ (500 μ M) to block the BK current component and determine the size of Cd²⁺-insensitive Kv currents was done after full recovery of the current at pHo 7.4 that required on average 3 min, most likely because of an equal lowering of intracellular pH (pHi) (not shown). Subtraction of the traces in Cd²⁺ from the traces at pHo 7.4 and 7.0 ultimately led to the BK current (Fig. 6b). As shown in the example of Fig. 6a, lowering pHo from 7.4 to 7.0 caused nearly 40% reduction of BK currents at all Ca²⁺ pre-loading steps injecting large amounts of Ca²⁺ ions into the cells (-20 to +40 mV). BK current peaks measured at pHo 7.4 followed the bell-shaped curve expected for BK channels (Marty & Neher, 1985; Neely & Lingle, 1992) and the same bell-shape of lower amplitude was evident at pHo 7.0 (Fig. 6c). No shift of the peak values was evident, indicating that the effect of lowering pHo cannot be attributed to a specific effect on L- or non-L-type Ca²⁺ channels.

We then determined the V-dependence of BK channel activation by measuring the BK currents following 100 ms pre-pulse to +20 mV at test pulses of increasing amplitude from -60 to +120 mV

by steps of 20 mV (Fig. 7a). Lowering pH_o caused a marked decrease of BK currents that were quantified by subtracting the K_v currents remaining after application of 500 μM Cd²⁺. Accordingly, the voltage-dependence of the normalized BK conductance, g_{BK}, was determined and data were fit by a Boltzmann function (see legend). As expected, pH_o 7.0 decreased by ~40% the maximal conductance compared to control (n = 8; P < 0.01, paired Student's t test). There was also a steeper V-dependence, with a decrease in the slope factor k in the Boltzmann equation from 33.8 mV (pH_o 7.4) to 28.4 mV (pH_o 7.0) for an e-fold change and a marked left shift of the half-maximal activation voltage (V_{1/2} = -61.0 and -49.9 mV, respectively). The two effects that most likely originate from the interaction of protons with the intracellular Ca²⁺ bowl sensor (Hou *et al.*, 2009) compensate each other to give a percentage of block of ~40% at nearly all potentials. Notice that, the left shift of g_{BK} at low pH_o is opposite to that of voltage-gated Na⁺, Ca²⁺ and K⁺ channels, suggesting a different action of protons on BK channel gating (see Discussion).

Given the strong effect of pH_o on g_{BK}, we also investigated its pH_o sensitivity over a wider range of pH_o (from 7.8 to 6.6). As shown in Fig. 7c, BK currents decrease with lowering pH_o with an IC₅₀ at pH 7.0 and a Hill coefficient of 1.26, indicating one proton binding to the site controlling g_{BK} permeability. At pH_o 6.6, the BK current block is 65% at nearly all potentials with ~-24 mV left shift of V_{1/2}. This suggests a strong depressive action of low pH_o on BK channels due possibly to a dual action on channel permeability (Brelidze & Magleby, 2004) and Ca²⁺-sensitivity of channel opening (Hou *et al.*, 2009) through the titration of amino acid residues with IC₅₀ near neutral pH_o.

To complete the test on most expressed ion channels contributing to AP firing we checked also the action of low pH_o on voltage-gated K_v currents measured in the presence of Na⁺, Ca²⁺, BK and SK channel blockers (Fig. 7d). At variance with BK, the K_v currents exhibited steep V-dependence between -20 and +30 mV and were only slightly reduced at pH_o 7.0. On average K_v currents were depressed by ~10% at voltages of maximal activation (+60 mV), with no evident shift to the voltage of half-maximal activation (Fig. 7e).

As previously shown, SK channels are functionally coupled to Cav1.3 channels in MCCs and control resting membrane potential, firing frequency and terminate burst firing (Vandael *et al.*, 2012). Given that total Cav currents and, particularly, Cav1 currents were little affected at pH_o 7.0 (Fig. 5d), we tested also whether SK channels undergo gating changes at acidic pH_o. Fig. 7f shows that when fully activated by Ca²⁺-loading steps of 250 ms to +20 mV, the amplitude and time course of the slowly decaying inward tail SK currents during step repolarization to -100 mV were nearly unchanged at pH_o 7.0. This suggests that lowering pH_o does not alter the number of functioning SK channels and their Ca²⁺-dependence.

Mixtures of BK and TASK-1 channel blockers mimic the action of low pH_o

Given the strong blocking effects of low pH_o on g_{BK} (Figs. 6, 7) and the key role that BK channels play in the repolarization phase of APs in MCCs (Marcantoni *et al.*, 2010; Martinez-Espinosa *et al.*,

2014), we hypothesized that combined block of BK and TASK channels (Fig. 3) could account for most of the action of low pHo on burst firings. To confirm this, we first determined the concentration of paxilline that blocks 50 to 70% of BK channels (Zhou & Lingle, 2014), thus reproducing the effects of low pHo. Using increasing concentrations (0.1 to 1.0 μM) we found that by holding MCCs at -70 mV, 100 and 300 nM paxilline induced 70 and 100% block of BK currents after nearly 180 and 60 s, respectively (Li & Cheung, 1999). Given that paxilline blocks BK channels exclusively in their closed state (Zhou & Lingle, 2014) and that the rate and degree of block is largely attenuated at more positive voltages, we expected that 100 and 300 nM could well fit the blocking conditions of BK channels at pHo 6.6 when MCCs are free to fire between V_{rest} of -48 mV and mean overshoots of +20 mV. We then tested whether mixtures of paxilline and A1899 could mimic the sustained burst firing induced by low pHo. We found that the best burst firing conditions were obtained when 300 nM paxilline were added to 300 nM A1899. Fig. 8 shows how addition of 300 nM A1899 to a spontaneously tonic firing MCC (top-left grey panel) causes mild cell depolarization (~ 6 mV) and intermittent burst firing activity (top-middle panel). Further addition of 300 nM paxilline converts the intermittent bursts into more regular, well-organized bursts (top-right panel). As previously reported (Marcantoni *et al.*, 2010), paxilline caused only small depolarization when applied on spontaneously firing MCCs (2-3 mV). These small depolarizations that sum to the depolarizing effects of TASK1-3 blockers may account only partially for the net increase of burst firing activity. The major action of paxilline on cell firing is most likely associated with the block of BK currents that sustain APs repolarization and counter balance the inward currents sustaining the plateau potential of bursts.

Quantitative analysis of burst firing at pHo 6.6, with A1899 and paxilline alone or mixtures of the two blockers at pHo 7.4 allowed direct comparison of the different firing conditions. Therefore, we estimated the mean \pm SEM of six parameters that best define burst firing properties: number of events per burst, burst duration, peak amplitude of 1st AP, peak amplitude of last AP, plateau amplitude and bursts frequency (Fig. 9). Restrictive tests of significance (** $P < 0.01$, one-way ANOVA) of all the parameters at pHo 6.6 compared with those estimated for 300 nM A1899, 1 μM paxilline and 300 nM A1899 + 300 nM paxilline indicate that the best mimicking firing conditions are those induced by the mixture of the two blockers (2nd column to the left). Under these conditions, 5 out of 6 parameters were not significantly different from those at pHo 6.6, while paxilline and A1899 alone changed more parameters (2 out of 6 parameters changing significantly). In conclusion, blocking of TASK or BK channels alone is sufficient to produce burst firing similar to that induced by sustained cell depolarization. This latter induces slow inactivation of the Nav channels that is sufficient to induce burst firing in MCCs (Vandael *et al.*, 2015b). However, simultaneous block of TASK and BK channels ensures more stable and regular burst firings. Critical to this is the block of BK channels that regulate the strength and duration of the fast after-hyperpolarization (AHP) phase

of APs (Prakriya & Lingle, 1999; Marcantoni *et al.*, 2010; Vandael *et al.*, 2010; Martinez-Espinosa *et al.*, 2014).

Cav1 channels contribute to burst firing at low pH_o: nifedipine attenuates and blocks while BayK8644 favours the bursts

The plateau phase of AP bursts in MCCs has been shown to be the result of a balance between Ca²⁺ entry through Cav channels and K⁺ exit through Kv, BK and SK channels (Vandael *et al.*, 2015b). We also showed that Cav currents during bursts are of lower amplitude compared to those passing during an AP but persist for the entire duration of the burst, thus sustaining enhanced neurotransmitter release during bursts (see fig. 10 in Vandael *et al.*, 2015b). An unresolved issue of burst firing in MCCs is how critical are Cav1 channels in burst production given that they sustain spontaneous firing in MCCs. This is particularly true for the Cav1.3 isoform which activates at more negative potentials than any other high-threshold Ca²⁺ channel and inactivates very slowly in MCCs (Marcantoni *et al.*, 2010; Vandael *et al.*, 2010). With the purpose of highlighting the role of Cav1 channels in burst generation, we tested the effects of increasing concentrations of nifedipine (0.1, 0.3, 1 and 3 μM) on burst firing. We found that even 100 nM nifedipine, which blocks ~50% of Cav1 currents in MCCs at -40 mV resting potential (Mahapatra *et al.*, 2011), was sufficient to convert the bursts into irregular tonic firing. Increasing doses of nifedipine (300 nM) accelerated the conversion and lowered the tonic firing frequency. Full block of the activity occurred at 3 μM. Fig. 10 recapitulates these observations. As shown, the current-clamped MCC displays a mild burst firing at control (top-left panel), which was converted in an irregular burst firing after applying 300 nM A1899 + 300 nM paxilline, following a weak cell depolarization (from -43 to -40 mV). The small depolarization observed in this cell, most likely derives from a weak expression of TASK1-3 channels that may drive the resting cell near to burst firing. Regardless of this, the two blockers (mainly paxilline) induced sustained irregular bursts lasting 300-1000 ms followed by profound hyperpolarizations, sustained by robust activation of outward SK currents (arrows in the top-middle panel to the left). Addition of 300 nM nifedipine first converted the burst into an irregular tonic firing (top-middle panel to the right). After a mild depolarization, the firing stopped. Burst firing block persisted in the presence of 3 μM nifedipine (top-right panel). Addition of 3 μM nifedipine always (n= 5) blocked the firing regardless of any small depolarization or hyperpolarization that originate from the different functional coupling and expression density of L-type and SK channels (Vandael *et al.*, 2012).

Nifedipine (3 μM) was also very effective in blocking burst firing induced by low pH_o (7.0 to 6.6) regardless of whether the bursts were continuously generated near rest (-40 to -50 mV) as in Fig. 10 or after brief depolarizations in cells maintained silent with steady hyperpolarizations (V_h -70 mV). Fig. 11 shows an example of MCC maintained at -70 mV that undergoes normal tonic firing at pH_o 7.4 during brief current injection of 100 ms (black trace). Tonic firing stops on cell repolarization (top-right inset), while the cell undergoes burst firing at pH_o 6.6 that persists after the

brief depolarization (red trace). Addition of 3 μM nifedipine stops the bursts and the cell repolarizes back to V_h (blue trace). We observed this in $n=12$ cells regardless of whether lowering pH_o ($n=7$) or applying mixtures of the two blockers ($n=5$) (not shown).

Given the involvement of Cav1 channels in burst firing generation, we tested whether increasing Cav1 channel currents with BayK8644 was sufficient to induce burst firing in MCCs. We previously reported that addition of 1 μM BayK8644 caused resting cell hyperpolarization and increased firing frequency (Marcantoni *et al.*, 2010), but we did not specifically investigate whether potentiation of Cav1 currents could generate tonic or burst firing in MCCs. We thus tested whether increasing doses of BayK8644 (0.1, 0.3 and 1 μM) favour burst firing in MCCs at pH_o 7.4. We found that in the majority of MCCs (7 out of 11) with resting irregular tonic activity BayK8644 induced burst firing even at concentrations as low as 0.1 μM while in the remaining 4 cells the DHP agonist induced only a marked frequency increase with no bursts. Fig. 12 shows two examples of MCCs responding differently to BayK8644. In panel **a**, BayK8644 induces burst firing whose duration progressively increase with increasing concentration. In panel **b**, BayK8644 progressively increases the AP firing frequency without inducing burst firings. Interestingly, in five MCCs that exhibited mild spontaneous burst firing at rest, BayK8644 converted the firing in to sustained bursts, causing depolarization blocks of several seconds in some case (not shown). In conclusion, Cav1 channels appears critical not only in regulating pacemaking in chromaffin cells (Marcantoni *et al.*, 2010; Vandael *et al.*, 2010; Vandael *et al.*, 2012) but also in contributing to burst firing.

Low pH_o -induced burst firing potently increases CA secretion in MCCs

A straightforward expectation of the resting depolarization and spontaneous burst firing induced by low pH_o is a net increase of Ca^{2+} entry through Cav channels that likely drives a marked increase of CA release from MCCs. We have previously shown that this occurs when burst firing is induced by application of TTX that reduces Na^+ currents through Nav1.3/Nav1.7 channels in MCCs (Vandael *et al.*, 2015b). Under these conditions, we have demonstrated that the oxidative charges accumulated during CA release increase more or less with the same proportion of Ca^{2+} charges increase through Cav channels (~ 3.5 -fold; Fig. 8 in Vandael *et al.*, 2015b). We thus expected that low pH_o exerts a similar boosting action on exocytosis and tested whether sustained burst firings induced by low pH_o or mixtures of TASK and BK channel blockers induce marked increases of CA release. To test this, we combined current-clamp recordings with CFE amperometry to reveal fast quantal release of CAs and determine how different firing patterns of 60 s at control (pH_o 7.4), low pH_o (6.6) or application of 300 nM A1899 + 300 nM paxilline affect CA secretion (Fig. 13).

Given the critical conditions of simultaneously recording AP firing (with a patch-pipette) and amperometric signals (with a CFE; see Materials & Methods), experiments at pH_o 6.6 and with TASK and BK channel blockers were carried out on different cells. MCCs were bathed in control solution (pH_o 7.4) and then perfused with the test solution (pH_o 6.6 or blockers) having the

precaution of changing the bath without moving the CFE. Fig. 13 a-c show three examples of recordings in MCCs maintained at control (pH_o 7.4, black traces), pH_o 6.6 (blue traces) or in the presence of 300 nM A1899 + 300 nM paxilline (red traces). At pH_o 7.4, the spontaneous tonic firing of MCCs in 2 mM extracellular Ca²⁺ induces basal release of CA in forms of amperometric spikes of very low frequency. A similar basal release in 2 mM Ca²⁺ has been observed, both in isolated BCCs and MCCs of adrenal gland slices (Picollo *et al.*, 2016). In ten MCCs all spontaneously firing, three cells had no amperometric spike activity while the remaining had rare spike events, casually distributed during a recording period of 60 s. Mean spike frequency was 0.02 ± 0.01 Hz (Fig. 13d). The frequency of spike events increased drastically at pH_o 6.6 (0.11 ± 0.3 Hz; $P < 0.01$, $n = 8$) and in the presence of TASK and BK channel blockers (0.18 ± 0.3 Hz; $P < 0.001$, $n = 8$).

Despite the marked increase in the rate of release, low pH_o and mixtures of the two blockers had no significant effects on the waveform of amperometric spikes (Fig. 13d). The parameters associated with the peak amplitude (I_{max}), time to peak (t_p), half-width ($t_{1/2}$), total quantity of charge released (Q) and cubic root of Q ($Q^{1/3}$) (as an estimate of vesicle size) remained unchanged with respect to control ($P > 0.05$). The significantly larger increase in I_{max} observed only with the two blockers ($P < 0.05$; middle-left panel) may derive from different mechanisms which could be due to: 1) an increased probability of double fusion of secretory events favoured by the 8-fold increased rate of vesicle release. 2) an increased probability of fused vesicles of larger size that coexist with a second population of smaller size vesicles in MCCs (Grabner *et al.*, 2005; Marcantoni *et al.*, 2009) and, 3) to a not well-identified interaction of protons with chromogranin A, a major protein in the vesicle that regulates the fraction of CA bound to the matrix (Jankowski *et al.*, 1993). This latter effect, however, occurs only at very acidic pH_o (5.5). Interestingly, because of the increased rate of release, the time course of cumulative secretion (black trace in Fig. 13e) exhibited a steeper rise at low pH_o (blue trace) that increased further with A1899 + paxilline (red trace). The mean quantity of cumulative charges recorded during 60 s recordings increased 7.4- and 11.6-fold with respect to control, respectively (Fig. 13d).

Given the opportunity of simultaneously recording AP bursts and secretory events, we tested specifically for a direct correlation between burst firing and amperometric spikes and found no specific links between the two signals. We were unable for instance to detect any frequency correlation between AP firing and secretory events. In the case of bursts, the AP frequency was uniform during 60 s of recordings (red burst firing trace of Fig. 13c) while in the case of spike events the frequency was rather irregular, alternating periods of high activity to long periods of no activity (red spike events trace of Fig. 13c). As previously reported, this suggests weak correlation between AP and amperometric events under both tonic and burst firing (Zhou & Mislser, 1995).

Discussion

We provided evidence that lowering pH_o causes a marked resting membrane depolarization, a switch of spontaneous firing from tonic to burst and a 7.4-fold increase of cumulative CA release in MCCs. The consequence of lowering pH_o is thus a non-neurogenic large increase of adrenaline and noradrenaline that is mainly driven by the increased Ca^{2+} entry during the plateau potential of bursts. From a functional point of view, we have shown that, by directly sensing a decrease of pH_o , MCCs act as pH sensors and secrete large amounts of CAs. This is the typical body response to recover from blood acidosis and hyperkalemia-induced muscle fatigue (Clausen, 1983) during heavy exercise (Medbo & Sejersted, 1990).

Specifically, we have shown that the marked resting membrane depolarization and burst firing induced by lowering pH_o from 7.4 to 6.6 is not exclusively associated with the block of pH-sensitive TASK-1 and TASK-3 K^+ channels but involves also a pH-induced block of Ca^{2+} - and V-dependent K^+ conductances (BK and Kv) that contribute further to the MCC depolarization at low pH_o . A blocking effect of low pH_o on the M-current (I_M) and TRPM4 channels that are expressed in CCs of some species and potentially contribute to the resting potential (Wallace *et al.*, 2002; Mathar *et al.*, 2010), can also not be excluded. In a preliminary series of experiments, we found that block of Kv7 channels by increasing doses of the selective blocker XE991 (0.3, 1 and 3 μM) (Wang *et al.*, 1998) caused partial hyperpolarization followed by cell depolarization and increased firing frequency. This suggests that MCCs express Kv7 (I_M) channels that could contribute to cell depolarization when blocked by protons. The possibility that Kv7 play a role on MCCs spontaneous firing is of great interest and further experiments are currently in progress.

Our findings clearly show that block of TASK-1 and TASK-3 is not the only mechanism supporting membrane depolarization and burst firing in MCCs. We have previously shown that burst firing in MCCs derives from the fine equilibrium between inward and outward currents flowing during AP repolarization (Vandael *et al.*, 2015b). As inward currents are mainly carried by Nav1.3/Nav1.7 and Cav1/Cav2 channels and outward current by BK, SK and Kv channels in MCCs, any significant increase of the former and decrease of the latter may potentially induce burst firing and increased Ca^{2+} entry. In the case of low pH_o , we found that a marked block of BK channels accompanied with a small attenuation of Cav channels is likely the cause of driving spontaneous tonic AP firing into regular burst firing. We have also shown that by blocking BK channels with paxilline to a cell already depolarized with saturating doses of A1899 we could induce regular burst firing, while adding increasing doses of the Cav1 blocker nifedipine 0.1 to 1 μM) we could revert the firing to a tonic mode. A critical involvement of Cav1 channels in burst firing is also supported by the potentiating effects of BayK8644 that in a large fraction of MCCs induce burst firing of increased durations in a dose-dependent manner.

Block of TASK channels does not account for the full effect of low pH_o on MCCs excitability

Our findings show clearly that widely used selective blockers of the two-pore TASK-1 and TASK-3 background channels (A1899 and PK-THPP) (Cotten, 2013; Bayliss *et al.*, 2015; Chokshi *et al.*,

2015; Dadi *et al.*, 2015) cause a net depolarization of resting MCCs. The depolarization is accompanied by an increased rate of AP firing and a moderate burst firing activity (Fig. 3). Comparing these effects with the selectivity of the two blockers, we can safely conclude that MCCs express more functional TASK-1 than TASK-3 “leak” channels and we cannot exclude that the attenuated effects of PK-THPP on resting potential could derive from a partial block of the TASK-1 isoform. That TASK-1 channels are the most likely expressed two-pore leak channels in MCCs is also suggested by the IC_{50} of the pH-induced resting depolarization (IC_{50} 7.2; Fig. 1c), which is very close to the pKa of protons block of homodimeric TASK-1 channels (pKa 7.4) and quite different from the pKa of homodimeric TASK-3 channels (pKa 6.7) reported by Bayliss *et al.*, 2015. It is also likely that MCCs express heterodimeric TASK1:TASK3 channels. This is suggested by the increased depolarization induced by the simultaneous application of A1899 and PK-THPP (Fig. 3d) and by the pKa of protons block of heterodimeric TASK1:TASK3 channels (pKa 7.2) that is similar to the IC_{50} of pH-induced MCCs depolarization.

It is interesting to note that TASK-3 are weakly or not expressed in RCCs (Inoue *et al.*, 2008) and BCCs (Enyeart *et al.*, 2004), while TASK-1 channels are highly expressed and mediate the muscarine-induced resting depolarization that induces increased CA secretion in RCCs (Inoue *et al.*, 2008). Concerning the size of the mean depolarization (~5 mV) induced by A1899 (Fig. 3c), it is worth remarking that this is likely an underestimation of the true depolarizing effects of TASK-1/TASK-3 channels block. This is due to the presence of highly expressed Ca^{2+} -dependent SK and BK channels (Vandael *et al.*, 2015a) that could partially attenuate the depolarizing effects of TASK-1/TASK-3 channels block. An increased Ca^{2+} influx during cell depolarization, which may occur at rest through open Cav1.3 channels, would induce partial hyperpolarization through the activation of SK and BK channels. Both channels contribute to set the resting potential of MCCs. It is worth recalling that selective block of SK channels by apamin (Vandael *et al.*, 2012) and BK channels by paxilline (Marcantoni *et al.*, 2010) induce net depolarizations of 2-3 mV at rest, in each case.

Given the existence of several K^+ channels regulating the resting membrane potential in MCCs (SK, BK, K_v) (Vandael *et al.*, 2015a), it is evident that the main role of pH-sensitive TASK channels at low pH_o is to trigger a sufficient cell depolarization that increases the rate of AP firing in spontaneously active MCCs. Further depolarizations and corresponding changes in regular burst firing are caused by the pH_o -induced inhibition of BK and partially of K_v rather than SK channels. These latter are nearly not affected by low pH_o (Fig. 7) and are thus expected to counteract rather than supporting the pH_o -induced depolarization, mostly because of the increased Ca^{2+} -entry induced by the TASK channels block. SK channels are fundamental in MCCs to terminate the bursts and allow the cell to recover Cav1 and TTX-sensitive Nav1.3/1.7 channels to initiate the following burst (Vandael *et al.*, 2015b).

Our data indicate that besides TASK-1 block a second major action of low pH_o is on BK channels, whose conductance is effectively inhibited at pH_o between 7.0 and 6.6 (Peers & Green, 1991) and

by similar changes of pH_i in various tissues (Cook *et al.*, 1984; Kume *et al.*, 1990). In the case of MCCs, a smaller contribution of BK currents to the repolarization phase of AP generation is critical to the generation of the plateau potential on top of which AP burst develops. To support this idea, we showed that the effects of pH_o 6.6 on firing modes can be mimicked by simply adding near saturating doses of paxilline to the TASK-1 blocker A1899. Indeed, the quantity of paxilline used (300 nM) is apparently higher than the quantity necessary to block 50% to 60% of BK channels, as it occurs at pH_o 6.6. However, paxilline block is state-dependent as it binds with high affinity to the closed state and with low affinity to the open state of the channel (Zhou & Lingle, 2014). Paxilline block is thus highly dependent on membrane potential, being strong at very negative potentials when channels are fully closed (IC_{50} 10 nM) and very weak at very positive potentials when channels are fully open (IC_{50} 10 μ M). Given this, we expect that in spontaneously firing cells in which the membrane potential fluctuates between -50 and +30 mV for most of the time, 300 nM paxilline would block around 50 to 60% of the BK channels. The higher amount of paxilline used would also account for the partial block of Cav channels that partially reduces the amount of Ca^{2+} entry and thus the number of activated BK channels (Prakriya & Lingle, 1999). Regardless of these considerations, there is still good correspondence between the effects of low pH_o and the two channel blockers. This combination indeed turns out to be essential to separate the effects of low pH_o on cell excitability (mimicked by the two blockers) from the action of protons on the molecular and subcellular components regulating the Ca^{2+} -driven CA release (see below).

The role of BK channels in burst firing

Our data show clearly that in addition to the blocking effects on TASK-1 and TASK-3 channels low pH_o has also marked effects on the BK channel conductance in the range between pH_o 7.0 and 6.6. Taking pH_o 7.0 as a reference pH_o , here we demonstrate that the other voltage- and Ca^{2+} -gated channels contributing to AP generation in MCCs (Nav, Kv, Cav and SK) are little or mildly affected at pH_o 7.0 compared to BK channels. The size and kinetics of Na^+ currents, carried by TTX-sensitive Nav channels in MCCs (Vandael *et al.*, 2015b), are little affected at pH_o 7.0. This is in line with the common notion that protons block of the negatively charged glutamic and aspartic acid residues in the outer pore selectivity filter of Na^+ channels require pH_o lower than 6.0 to significantly reduce channel permeability (Catterall, 2000). The same is true for the Ca^{2+} currents carried by Cav1.2, Cav1.3, Cav2.1, Cav2.2 and Cav2.3 in MCCs (Marcantoni *et al.*, 2010; Mahapatra *et al.*, 2011) that are mildly attenuated at pH_o 7.0. The Cav1 and Cav2 channels selectivity filter is formed by a ring of four negatively charged glutamic acid residues (Heinemann *et al.*, 1992), whose partial protonation requires more acidic pH_o to effectively reduce Ca^{2+} permeability. Also the protonation of membrane surface charges responsible for the right shift of $gCa(V)$ requires more acidic pH to produce large effects (Zhou & Jones, 1996). The voltage-dependent activation of Cav channels is only slightly affected (Fig. 5a) and the same is true for the

time-course of the Ca^{2+} -dependent inactivation of L-type channels which is not significantly altered at pH_o 7.0 during depolarizations that mimic the mean burst duration (300 ms).

Concerning the effects of pH_o 7.0 on SK channels, we found also no evidence for a block of SK currents, which is consistent with the notion that SK channels are voltage-independent and their open probability is steeply dependent on $[\text{Ca}^{2+}]_i$, with an EC_{50} of $\sim 0.5 \mu\text{M}$ (Fakler & Adelman, 2008). Such high affinity for Ca^{2+} is due to the presence of calmodulin (CaM) Ca^{2+} -binding sites, whose occupation regulates the Ca^{2+} -CaM-dependent conformational changes driving SK channel open probability (Keen *et al.*, 1999). To compete effectively with Ca^{2+} for the occupancy of these sites, the intracellular proton concentrations must be at least 10- to 100-fold higher than the EC_{50} for Ca^{2+} . Given this, even under a sizable proton permeation through the plasmalemma, pH_i should have to drop below 6.0 to have sizeable effects on SK open probability.

At variance with the other channels, low pH_o has a marked inhibitory effect on BK channels conductance. The inhibition is characterized by a marked current depression at nearly all potentials when BK channels are either activated by a fixed (Fig. 7b) or variable Ca^{2+} loading (Fig. 6c). Inhibition of BK channels by protons occurs through a reduction of $g_{\text{BK}}(V)$ at all potentials and a marked shift of the curve toward negative potentials with not significant changes of the V -dependence (Fig. 7b). This is in agreement with the reported effects of low pH_o on the BK channels of type-I carotid body cells (Peers & Green, 1991) and low pH_i on the BK channels of rabbit trachea smooth muscle (Kume *et al.*, 1990). Our data are also in line with the widely accepted notion that low pH_o (or low pH_i) acts on BK channels by mainly decreasing their open probability in the pH range between 7.8 and 6.4 in variety of cells (Cook *et al.*, 1984; Christensen & Zeuthen, 1987; Schubert *et al.*, 2001). On this issue, there is a general agreement that hydrogen ions decrease the open probability of BK channels by shortening their open state but how this occurs it is still matter of discussion (Hou *et al.*, 2009). We have not specifically tested whether changes of pH_o could induce comparable changes to pH_i , but two key considerations suggest that this is likely the case. Lowering of pH_o in rat chromaffin cells of adrenal gland cause a rapid fall of intracellular pH_i (Fujiwara *et al.*, 1994). In our experiments on BK channels, the onset of low pH_o effects required usually 20-40 s to reach steady-state effects while washing out was complete in not less than 3 min (see Materials & Methods). Block of BK channel permeability by protons also occurs, but at significantly more acidic pH (pK_a 5.1) (Brelidze & Magleby, 2004).

Cav1 channels contribute to the low pH_o induced burst firing

Cav1.3 channels possess all the gating properties to regulate resting potential and sustain burst firing in chromaffin cells. They activate at relative low membrane voltages in 2 mM Ca^{2+} and deactivate slowly (Koschak *et al.*, 2001; Marcantoni *et al.*, 2010), are effectively coupled to BK channels (Prakriya & Lingle, 1999; Vandael *et al.*, 2010), and are likely to contribute significantly to the inward Ca^{2+} current that critically sustains burst durations of 200 to 500 ms at depolarized potentials (-30 to -20 mV) (Vandael *et al.*, 2015b). Here we have shown that low doses of nifedipine

(100 to 300 nM), which produce only partial block of L-type channels (40 to 60% at resting potentials, Mahapatra *et al.*, 2011), is sufficient to revert the bursts into tonic firing. Nifedipine is also effective in preventing bursts that are generated by step depolarization from very negative V_h (-70 mV). Under these conditions, nifedipine blocks the burst that persists when the cell is repolarized, but not the tonic firing during the depolarization that is sustained by the available Nav1.3/Nav1.7 and Cav2 channels recruited at negative V_h . Finally, a role for Cav1 channels in burst firing is also suggested by the potentiating effects of BayK8644 that is very effective in inducing burst firing in a fraction of MCCs that most likely possess higher densities of Cav1 channels or lower densities of BK and SK channels. Both conditions are at the basis of increased MCCs excitability either in form of higher tonic firing frequencies (Vandael *et al.*, 2012), increased burst firing and depolarization block (Vandael *et al.*, 2010).

Tonic-to-burst firing is the main “motor” of the increased CA secretion at low pH_o

An important finding of our work is that low pH_o causes a marked increase of CAs release during resting conditions in MCCs (Fig. 13e). This is in good agreement with previous observations in RCCs (Inoue *et al.*, 2008), where lowering of pH_o is reported to induce an increased rate of AP firing and a consequent increase of released CAs. Our data also in good agreement with reports on MCCs (Vandael *et al.*, 2015b) and RCCs (Zhou & Mislser, 1995; Duan *et al.*, 2003), in which burst firing is shown more effective in potentiating CAs release than increasing the rate of AP firing. In the case of MCCs, burst firing was induced by blocking Nav1.3/av1.7 channels with TTX, and produced a 3.7-fold increase of cumulative charges associated with released CAs, in good correlation with the 3.5-fold increase of Ca^{2+} entering the cells during bursts. In the case of pH_o 6.6, the increase of cumulative charges associated with CA secretion is even more marked (7.4-fold). This larger value is likely to derive from the different protocols used to generate APs rather than to specific effects of pH_o on secretion. In the present work we maintained the cells at their physiological resting potential (-45 to -50 mV) while measuring amperometric signals. Previously, we first hyperpolarized the cells to -70 mV to recruit most available Ca^{2+} channels and then depolarized the cell to -50 mV with square current pulses (Vandael *et al.*, 2015b). Thus, with the present protocol, there are less available Ca^{2+} channels at rest and the basal secretion in control condition is significantly smaller with respect to the previous protocol. A second reason for the larger increase of cumulative charges is that pH_o 6.6 and the TASK and BK channel blockers induce more regular burst firing during the time of amperometric recordings. Bursts at pH_o 6.6 are not interposed with APs of high frequency as in the case of Nav13/Nav1.7 block (see Fig. 10b in (Vandael *et al.*, 2015b).

Our data also helps clarifying how much of the marked enhancement induced by low pH_o is associated with the switch from tonic to burst and how much is due to an interaction of protons with the secretory apparatus (vesicle loading, kinetics of vesicle fusion and CA release). Our findings show that the enhanced secretion by low pH_o is attributable mainly to switch from tonic to burst

firing rather than to an effect of pH_o on the secretory apparatus itself. Application of A1899 and paxilline that mainly act on ionic conductances produces even larger increases of cumulative charges associated with released CAs (11.6-fold). In addition to this, the effects of low pH_o nicely compare with those of the two blockers. Low pH_o and blockers increase significantly the rate of amperometric events while have nearly no effects on the parameters associated with the shape of amperometric spikes, with the exception of I_{max} with the two blockers that we have previously underlined. Thus, the common cause of enhanced secretion is the marked increase of Ca^{2+} entering the cells during the sustained bursts during either low pH_o or A1899 + paxilline application. A final interesting finding of our study is that even under sustained burst firing induced by low pH_o or TASK and BK channel block there is no clear evidence of synchronism between AP firing and amperometric spikes. In other words, most Cav channels are not co-localized with secretory vesicles in CCs and Ca^{2+} has to diffuse inside the cell to trigger most of the exocytotic events (Klingauf & Neher, 1997).

The physiological role of sensing low pH_o in the regulation of blood acidosis and hyperkalemia

Adrenal CCs respond to acidosis and hyperkalemia with increased firing activity and release of adrenaline (Kao *et al.*, 1991; Fujiwara *et al.*, 1994; Inoue *et al.*, 2008; Mahapatra *et al.*, 2011). This occurs typically during heavy exercise and, together with the CAs released from sympathetic nerve terminals, is at the basis of the key body response to recover from muscle fatigue (Medbo & Sejersted, 1990). Besides increasing heart beat rates and adapting all other functions involved in the “fight-or-flight” body response, the elevation of circulating CAs increases the levels of cAMP in fatigued skeletal muscles through β_2 -adrenergic receptors stimulation (Clausen *et al.*, 1993). Elevated cAMP levels increase the phosphorylation of Na^+/K^+ ATPase pumps with consequent decrease of K^+ concentration outside the sarcolemma. The body response to acidosis and hyperkalemia is fast, with restoration of the plasma $[K]_o$ to its physiological value (3.5 mM) within a few minutes after the interruption of intense muscle exercise while pH_o remains low (7.2 to 6.9) (see Fig. 6 in (Medbo & Sejersted, 1990)). pH_o returns to its normal plasma level (7.4) after ~1 h from the end of the exercise.

Here we have shown that at the basis of the body response to acidosis there is likely an effective pH sensing mechanism involving a marked increase of cell excitability and CA release from the CCs of the adrenal medulla. Chromaffin cells undergo pronounced depolarization and switches their tonic firing into bursts, which boosts Ca^{2+} entry and Ca^{2+} -driven CA release. A key point of our work is that this non-neurogenic response is likely to be mainly controlled by changes of ion conductances and cell excitability rather than by specific effects of pH_o on the secretory machinery, i.e., altered vesicle loading ((Borges *et al.*, 2010), formation of the fusion pore and secretion of vesicle content (Lindau & Alvarez de Toledo, 2003) or alteration of bound CA in the vesicle matrix (Jankowski *et al.*, 1993). The reported data represent also a nice example of how typical neuron-

like burst firings can be exploited by chromaffin cells to effectively control key physiological functions (Lingle, 2015).

References

- Barry PH. (1994). JPCalc, a software package for calculating liquid junction potential corrections in patch-clamp, intracellular, epithelial and bilayer measurements and for correcting junction potential measurements. *Journal of neuroscience methods* **51**, 107-116.
- Bayliss DA, Barhanin J, Gestreau C & Guyenet PG. (2015). The role of pH-sensitive TASK channels in central respiratory chemoreception. *Pflügers Archiv-European Journal of Physiology* **467**, 917-929.
- Berkefeld H & Fakler B. (2013). Ligand-gating by Ca²⁺ is rate limiting for physiological operation of BK(Ca) channels. *The Journal of neuroscience : the official journal of the Society for Neuroscience* **33**, 7358-7367.
- Borges R, Pereda D, Beltran B, Prunell M, Rodriguez M & Machado JD. (2010). Intravesicular factors controlling exocytosis in chromaffin cells. *Cell Mol Neurobiol* **30**, 1359-1364.
- Brelidze TI & Magleby KL. (2004). Protons block BK channels by competitive inhibition with K⁺ and contribute to the limits of unitary currents at high voltages. *The Journal of general physiology* **123**, 305-319.
- Carabelli V, Hernandez-Guijo JM, Baldelli P & Carbone E. (2001). Direct autocrine inhibition and cAMP-dependent potentiation of single L-type Ca²⁺ channels in bovine chromaffin cells. *Journal of Physiology-London* **532**, 73-90.
- Carabelli V, Marcantoni A, Comunanza V, De Luca A, Diaz J, Borges R & Carbone E. (2007). Chronic hypoxia up-regulates alpha(1H) T-type channels and low-threshold catecholamine secretion in rat chromaffin cells. *Journal of Physiology-London* **584**, 149-165.
- Catterall WA. (2000). From ionic currents to molecular mechanisms: the structure and function of voltage-gated sodium channels. *Neuron* **26**, 13-25.
- Catterall WA, Goldin AL & Waxman SG. (2005). International Union of Pharmacology. XLVII. Nomenclature and structure-function relationships of voltage-gated sodium channels. *Pharmacol Rev* **57**, 397-409.
- Cesetti T, Hernandez-Guijo JM, Baldelli P, Carabelli V & Carbone E. (2003). Opposite action of beta 1- and beta 2-adrenergic receptors on Ca(V)₁ L-channel current in rat adrenal chromaffin cells. *Journal of Neuroscience* **23**, 73-83.
- Chokshi RH, Larsen AT, Bhayana B & Cotten JF. (2015). Breathing Stimulant Compounds Inhibit TASK-3 Potassium Channel Function Likely by Binding at a Common Site in the Channel Pore. *Molecular pharmacology* **88**, 926-934.

- Christensen O & Zeuthen T. (1987). Maxi K⁺ channels in leaky epithelia are regulated by intracellular Ca²⁺, pH and membrane potential. *Pflugers Archiv : European journal of physiology* **408**, 249-259.
- Clausen T. (1983). Adrenergic control of Na⁺-K⁺-homoeostasis. *Acta medica Scandinavica Supplementum* **672**, 111-115.
- Clausen T, Andersen SL & Flatman JA. (1993). Na⁽⁺⁾-K⁺ pump stimulation elicits recovery of contractility in K⁽⁺⁾-paralysed rat muscle. *The Journal of physiology* **472**, 521-536.
- Coburn CA, Luo YF, Cui MX, Wang JB, Soll R, Dong JC, Hu B, Lyon MA, Santarelli VP, Kraus RL, Gregan Y, Wang Y, Fox SV, Binns J, Doran SM, Reiss DR, Tannenbaum PL, Gotter AL, Meinke PT & Renger JJ. (2012). Discovery of a Pharmacologically Active Antagonist of the Two-Pore-Domain Potassium Channel K2P9.1 (TASK-3). *Chemmedchem* **7**, 123-133.
- Cook DL, Ikeuchi M & Fujimoto WY. (1984). Lowering of pHi inhibits Ca²⁺-activated K⁺ channels in pancreatic B-cells. *Nature* **311**, 269-271.
- Cotten JF. (2013). TASK-1 (KCNK3) and TASK-3 (KCNK9) tandem pore potassium channel antagonists stimulate breathing in isoflurane-anesthetized rats. *Anesth Analg* **116**, 810-816.
- Cryer PE. (1980). Physiology and pathophysiology of the human sympathoadrenal neuroendocrine system. *The New England journal of medicine* **303**, 436-444.
- Dadi PK, Luo B, Vierra NC & Jacobson DA. (2015). TASK-1 Potassium Channels Limit Pancreatic alpha-Cell Calcium Influx and Glucagon Secretion. *Mol Endocrinol* **29**, 777-787.
- Duan K, Yu X, Zhang C & Zhou Z. (2003). Control of secretion by temporal patterns of action potentials in adrenal chromaffin cells. *The Journal of neuroscience : the official journal of the Society for Neuroscience* **23**, 11235-11243.
- Enyeart JA, Danthi SJ & Enyeart JJ. (2004). TREK-1 K⁺ channels couple angiotensin II receptors to membrane depolarization and aldosterone secretion in bovine adrenal glomerulosa cells. *American journal of physiology Endocrinology and metabolism* **287**, E1154-1165.
- Fakler B & Adelman JP. (2008). Control of K-Ca channels by calcium nano/microdomains. *Neuron* **59**, 873-881.
- Fujiwara N, Warashina A & Shimoji K. (1994). Characterization of low pH-induced catecholamine secretion in the rat adrenal medulla. *Journal of neurochemistry* **62**, 1809-1815.

- Gavello D, Vandael D, Gosso S, Carbone E & Carabelli V. (2015). Dual action of leptin on rest-firing and stimulated catecholamine release via phosphoinositide 3-kinase-driven BK channel up-regulation in mouse chromaffin cells. *The Journal of physiology* **593**, 4835-4853.
- Grabner CP, Price SD, Lysakowski A & Fox AP. (2005). Mouse chromaffin cells have two populations of dense core vesicles. *Journal of Neurophysiology* **94**, 2093-2104.
- Heinemann SH, Terlau H, Stuhmer W, Imoto K & Numa S. (1992). Calcium channel characteristics conferred on the sodium channel by single mutations. *Nature* **356**, 441-443.
- Horn R & Marty A. (1988). Muscarinic activation of ionic currents measured by a new whole-cell recording method. *The Journal of general physiology* **92**, 145-159.
- Hou S, Horrigan FT, Xu R, Heinemann SH & Hoshi T. (2009). Comparative effects of H⁺ and Ca²⁺ on large-conductance Ca²⁺- and voltage-gated Slo1 K⁺ channels. *Channels (Austin, Tex)* **3**, 249-258.
- Inoue M, Fujishiro N & Imanaga I. (1998). Hypoxia and cyanide induce depolarization and catecholamine release in dispersed guinea-pig chromaffin cells. *The Journal of physiology* **507 (Pt 3)**, 807-818.
- Inoue M, Harada K, Matsuoka H, Sata T & Warashina A. (2008). Inhibition of TASK1-like channels by muscarinic receptor stimulation in rat adrenal medullary cells. *Journal of neurochemistry* **106**, 1804-1814.
- Jankowski JA, Schroeder TJ, Ciolkowski EL & Wightman RM. (1993). Temporal characteristics of quantal secretion of catecholamines from adrenal medullary cells. *The Journal of biological chemistry* **268**, 14694-14700.
- Kao LS, Ho MY & Cragoe EJ, Jr. (1991). Intracellular pH and catecholamine secretion from bovine adrenal chromaffin cells. *Journal of neurochemistry* **57**, 1656-1660.
- Keen JE, Khawaled R, Farrens DL, Neelands T, Rivard A, Bond CT, Janowsky A, Fakler B, Adelman JP & Maylie J. (1999). Domains responsible for constitutive and Ca(2+)-dependent interactions between calmodulin and small conductance Ca(2+)-activated potassium channels. *The Journal of neuroscience : the official journal of the Society for Neuroscience* **19**, 8830-8838.
- Klingauf J & Neher E. (1997). Modeling buffered Ca²⁺ diffusion near the membrane: Implications for secretion in neuroendocrine cells. *Biophysical journal* **72**, 674-690.
- Koschak A, Reimer D, Huber I, Grabner M, Glossmann H, Engel J & Striessnig J. (2001). alpha 1D (Cav1.3) subunits can form L-type Ca²⁺ channels activating at negative voltages. *Journal of Biological Chemistry* **276**, 22100-22106.

- Kume H, Takagi K, Satake T, Tokuno H & Tomita T. (1990). Effects of intracellular pH on calcium-activated potassium channels in rabbit tracheal smooth muscle. *The Journal of physiology* **424**, 445-457.
- Li G & Cheung DW. (1999). Effects of paxilline on K⁺ channels in rat mesenteric arterial cells. *Eur J Pharmacol* **372**, 103-107.
- Lindau M & Alvarez de Toledo G. (2003). The fusion pore. *Biochim Biophys Acta* **1641**, 167-173.
- Lingle CJ. (2015). NAVigating a transition from single action potential firing to bursting in chromaffin cells. *The Journal of physiology* **593**, 761-762.
- Mahapatra S, Marcantoni A, Vandael DHF, Striessnig J & Carbone E. (2011). Are Ca(v)1.3 pacemaker channels in chromaffin cells? Possible bias from resting cell conditions and DHP blockers usage. *Channels* **5**, 219-224.
- Marcantoni A, Carabelli V, Vandael DH, Comunanza V & Carbone E. (2009). PDE type-4 inhibition increases L-type Ca²⁺ currents, action potential firing, and quantal size of exocytosis in mouse chromaffin cells. *Pflugers Archiv-European Journal of Physiology* **457**, 1093-1110.
- Marcantoni A, Vandael DHF, Mahapatra S, Carabelli V, Sinnegger-Brauns MJ, Striessnig J & Carbone E. (2010). Loss of Cav1.3 Channels Reveals the Critical Role of L-Type and BK Channel Coupling in Pacemaking Mouse Adrenal Chromaffin Cells. *Journal of Neuroscience* **30**, 491-504.
- Marder E & Taylor AL. (2011). Multiple models to capture the variability in biological neurons and networks. *Nature Neuroscience* **14**, 133-138.
- Martinez-Espinosa PL, Yang C, Gonzalez-Perez V, Xia XM & Lingle CJ. (2014). Knockout of the BK beta2 subunit abolishes inactivation of BK currents in mouse adrenal chromaffin cells and results in slow-wave burst activity. *The Journal of general physiology* **144**, 275-295.
- Marty A & Neher E. (1985). Potassium channels in cultured bovine adrenal chromaffin cells. *Journal of Physiology-London* **367**, 117-141.
- Mathar I, Vennekens R, Meissner M, Kees F, Van der Mieren G, Camacho Londono JE, Uhl S, Voets T, Hummel B, van den Bergh A, Herijgers P, Nilius B, Flockerzi V, Schweda F & Freichel M. (2010). Increased catecholamine secretion contributes to hypertension in TRPM4-deficient mice. *The Journal of clinical investigation* **120**, 3267-3279.

- Medbo JI & Sejersted OM. (1990). PLASMA POTASSIUM CHANGES WITH HIGH-INTENSITY EXERCISE. *Journal of Physiology-London* **421**, 105-122.
- Nassar-Gentina V, Pollard HB & Rojas E. (1988). Electrical activity in chromaffin cells of intact mouse adrenal gland. *The American journal of physiology* **254**, C675-683.
- Neely A & Lingle CJ. (1992). Effects of muscarine on single-rat adrenal chromaffin cells. *Journal of Physiology-London* **453**, 133-166.
- Peers C & Green FK. (1991). Inhibition of Ca²⁺-activated K⁺ currents by intracellular acidosis in isolated type-I cells of the neonatal rat carotid-body. *Journal of Physiology-London* **437**, 589-602.
- Piccolo F, Battiato A, Bernardi E, Marcantoni A, Pasquarelli A, Carbone E, Olivero P & Carabelli V. (2016). Microelectrode Arrays of Diamond-Insulated Graphitic Channels for Real-Time Detection of Exocytotic Events from Cultured Chromaffin Cells and Slices of Adrenal Glands. *Anal Chem* **88**, 7493-7499.
- Prakriya M & Lingle CJ. (1999). BK channel activation by brief depolarizations requires Ca²⁺ influx through L- and Q-type Ca²⁺ channels in rat chromaffin cells. *Journal of Neurophysiology* **81**, 2267-2278.
- Schubert R, Krien U & Gagov H. (2001). Protons inhibit the BK(Ca) channel of rat small artery smooth muscle cells. *Journal of vascular research* **38**, 30-38.
- Streit AK, Netter MF, Kempf F, Walecki M, Rinne S, Bollepalli MK, Preisig-Muller R, Renigunta V, Daut J, Baukowitz T, Sansom MSP, Stansfeld PJ & Decher N. (2011). A Specific Two-pore Domain Potassium Channel Blocker Defines the Structure of the TASK-1 Open Pore. *Journal of Biological Chemistry* **286**, 13977-13984.
- Vandael DH, Marcantoni A & Carbone E. (2015a). Cav1.3 Channels as Key Regulators of Neuron-Like Firings and Catecholamine Release in Chromaffin Cells. *Curr Mol Pharmacol* **8**, 149-161.
- Vandael DH, Marcantoni A, Mahapatra S, Caro A, Ruth P, Zuccotti A, Knipper M & Carbone E. (2010). Ca(v)1.3 and BK Channels for Timing and Regulating Cell Firing. *Molecular Neurobiology* **42**, 185-198.
- Vandael DH, Ottaviani MM, Legros C, Lefort C, Guerineau NC, Allio A, Carabelli V & Carbone E. (2015b). Reduced availability of voltage-gated sodium channels by depolarization or blockade by tetrodotoxin boosts burst firing and catecholamine release in mouse chromaffin cells. *The Journal of physiology* **593**, 905-927.

- Vandael DHF, Zuccotti A, Striessnig J & Carbone E. (2012). Ca(V)1.3-Driven SK Channel Activation Regulates Pacemaking and Spike Frequency Adaptation in Mouse Chromaffin Cells. *Journal of Neuroscience* **32**, 16345-16359.
- Wallace DJ, Chen C & Marley PD. (2002). Histamine promotes excitability in bovine adrenal chromaffin cells by inhibiting an M-current. *The Journal of physiology* **540**, 921-939.
- Wang HS, Pan Z, Shi W, Brown BS, Wymore RS, Cohen IS, Dixon JE & McKinnon D. (1998). KCNQ2 and KCNQ3 potassium channel subunits: molecular correlates of the M-channel. *Science (New York, NY)* **282**, 1890-1893.
- Zhou W & Jones SW. (1996). The effects of external pH on calcium channel currents in bullfrog sympathetic neurons. *Biophysical journal* **70**, 1326-1334.
- Zhou Y & Lingle CJ. (2014). Paxilline inhibits BK channels by an almost exclusively closed-channel block mechanism. *Journal of General Physiology* **144**, 415-440.
- Zhou Z & Mislis S. (1995). Action potential-induced quantal secretion of catecholamines from rat adrenal chromaffin cells. *The Journal of biological chemistry* **270**, 3498-3505.

Competing interests: All authors declare no conflict of interest.

Author contributions

L.G. and D.H.F.V. contributed to data collection of whole-cell and amperometric experiments. V.C. contributed to the design, analysis and interpretation of amperometric measurements. L.G. and E.C. contributed to the conception and design of the experiments, data analysis, drafting the article as well as revising it critically for important intellectual content with the input of all co-authors. All authors have approved the final version of the manuscript.

Funding

This work was supported by the Italian MIUR (PRIN 2010/2011 project 2010JFYFY2); the University of Torino and Telethon Foundation (grant # GGP15110).

Acknowledgments

We thank Dr. C. Franchino for excellent technical assistance. Dr.s A. Marcantoni, C. Calorio and D. Gavello for a critical reading of the manuscript and helpful discussions. Special thanks goes to Dr. Chris Lingle for the continuous support, discussions and proofreading of the manuscript.

Figure legends

Fig. 1 - Low pH_o effects on spontaneous firing in MCCs. **a)** *Top*: representative trace of a current clamped spontaneously firing MCC (no current injection) at pH_o 7.4, 7.0 and 6.6. *Bottom*: AP recordings on an expanded time scale corresponding to the grey window above. A decrease in pH results in depolarization and the switch of firing modes from tonic (pH_o 7.4, grey rectangle to the left) to mildly bursting (pH_o 7.0, grey rectangle in the center), to sustained bursting (pH_o 6.6, grey rectangle to the right). Intermittent and sustained burst firing are accompanied by a net decrease of AP peak amplitude associated with the slow inactivation of Nav channels at depolarized potentials (Vandael *et al.*, 2015b). The dotted line indicates the 0 mV level. Dashed lines indicate V_{rest} at the different pH_o. V_{rest} was determined by averaging the slowly rising potential during the interspike interval. **b)** Mean firing rate at different pH_o obtained from n= 9 MCCs. **c)** Mean V_{rest} versus pH_o. The continuous curve is a dose-response best fit with equation: $V = V_{\min} + [(V_{\max} - V_{\min}) / (1 + 10^{-(\text{pH} - \text{IC}_{50})/n})]$ with V_{min}= -53 mV, V_{max}= -34 mV, IC₅₀= 7.2 and Hill slope n= 2.2 (n= 9 cells). **d)** Representative trace of the stability of the control firing recording and reversible effects of pH_o 6.6. The acidic solution was applied for 60 s to induce burst firing and then wash out to rescue the initial tonic firing frequency. The V_m of current-clamp recordings was not corrected for the LJPs (see Materials & Methods).

Fig. 2 – Analysis of tonic and burst firing patterns at different pH_o. *Top*: representative AP recordings at the indicated pH_o. *Middle*: ISI distribution for the indicated pH_o from a number of cells varying from n = 22 (pH_o 7.4) to n = 7 at pH_o 7.2. The continuous curves are best fits with double Gaussian functions with means (1st, 2nd) indicated in each panel. *Bottom*: joint ISI graphs obtained by plotting each ISI on the x-axis (ISL_i) against its successive ISI duration (ISL_{i+1}) on the y-axis. Irregular firing at various pH_o leads to a cloudy pattern, while burst firing at very low pH_o leads to an L-shaped distribution. The firing characteristics of the cells, i.e., the interspike interval, the AP frequency and the threshold were calculated as described in Vandael *et al.*, 2012 and Vandael *et al.*, 2015b.

Fig. 3 - Effects of the TASK-1 and TASK-3 blockers A1899 and PK-THPP on MCCs firing. a)

Representative traces of spontaneously firing MCCs in control conditions (pH_o 7.4) and during bath application of 300 nM PK-THPP (upper trace) or A1899 (lower trace) indicated by the horizontal bars. On top of each trace are shown 5 s of recordings on an expanded time scale corresponding to the grey window below. The dotted line indicates the 0 mV level. Dashed lines indicate V_{rest} at control (pH_o 7.4) and with the blocker. Notice the difference between the effects on firing rates and modes of the two blockers. **b, c)** Mean frequencies (Hz) and resting potential (mV) in control condition (dark bars), during addition of 300 nM PK-THPP, 300 nM A1899 or simultaneous application of the two blockers (**P < 0.01; ***P < 0.001; one-way ANOVA followed by a Bonferroni *post hoc* test). **d)** Representative trace of a spontaneously firing MCC at pH_o 7.4 to which A1899 (300 nM) was applied for 2 min alone and PK-THPP (300 nM) was added later to test the simultaneous effects of the two drugs. On top are shown 5 s of recordings on an expanded time scale corresponding to the grey window below. The V_m of current-clamp recordings was not corrected for the LJPs (see Materials & Methods).

Fig. 4 - Lowering pH_o to 7.0 has minimal effects on Nav currents in MCCs. a)

Whole cell Nav currents evoked by depolarizing steps lasting 10 ms in steps of 10 mV from -40 to +60 mV at pH_o 7.4 (black traces) and 7.0 (red traces). V_h was -70 mV. *Insets*: mean t_(90%-10%) and τ_{inact} at -20, -10 and 0 mV at pH_o 7.4 (black dots) and pH_o 6.6 (red dots). **b, c)** Normalized I_{Na} current amplitudes and g_{Na} versus voltage at pH_o 7.4 (black squares) and pH_o 7.0 (red squares) (n = 7). g_{Na}(V) was calculated as described in Materials and Methods. In **b** the normalized I/V curves are continuous lines drawn through data points. *Inset*: Mean I_{Na} peak values (n = 9) at 0 mV at pH_o 7.4 (black bar) and 7.0 (red bar). In **c** the two continuous curves are the results of the fit with two Boltzmann equations with half-maximal values V_{1/2} (in mV) and slope factors k (in mV) obtained from the fit: 17.6 mV and 4.9 mV (pH_o 7.4; black curve) and 16.6 mV and 4.8 mV (pH_o 7.0; red curve). The V_m of voltage-clamp recordings was not corrected for the LJPs (see Materials & Methods).

Fig. 5 - Lowering pH_o to 7.0 has little effect on calcium current amplitude. **a)** Overlapped whole cell recordings of total Ca²⁺ currents at the test potentials indicated, at pH_o 7.4 (black traces) and pH_o 7.0 (red traces; V_h = -70 mV). **b)** Current-voltage relationship at pH_o 7.4 (black dots) and pH_o 6.6 (red squares) of normalized Ca²⁺ currents. *Inset:* Mean I_{Ca} peak values (n = 8) at 0 mV at pH_o 7.4 (black bar) and 7.0 (red bar). **c)** Normalized Ca²⁺ channels conductance fit with a Boltzmann function: V_{1/2} = -16.2 mV, k = 7.1 mV at pH_o 7.4 (black dots and trace) and V_{1/2} = -12.0 mV, k = 7.0 mV for pH_o 7.0 (red squares and trace; n = 8). Notice the 4.2 mV shift of g_{Ca}(V) to the right at low pH_o. g_{Ca}(V) was calculated as described in Materials and Methods. **d)** Superimposed normalized whole-cell recordings of total and L-type calcium currents at -10 mV at pH_o 7.4 (black trace) and pH_o 6.6 (red trace) lasting 300 ms to estimate the time course of current inactivation. L-type currents were obtained by subtraction of nifedipine (3 μM) resistant current from control traces. The continuous yellow curves within traces of total Cav currents are double exponential fits with the following parameters: A_{fast} = -22.2 pA, A_{slow} = -24.2 pA, τ_{fast} = 16.4 ms, τ_{slow} = 229.3 ms C = -32.4 pA at pH_o 7.4 and, A_{fast} = -25.3, A_{slow} = -23.5, τ_{fast} = 18.6 ms, τ_{slow} = 208.6 ms C = -29.5 pA at pH_o 7.0. The continuous yellow curves within traces of L-type currents are single exponential fits with the following parameters: A_{fast} = -19.5 pA, τ_{fast} = 39.9 ms at pH_o 7.4 and, A_{fast} = -19.0, τ_{fast} = 32.5 ms, at pH_o 7.0. The V_m of voltage-clamp recordings was not corrected for the LJPs (see Materials & Methods).

Fig. 6 - Lowering pH_o to 7.0 reduces markedly the size of BK currents. **a)** Total K⁺ currents (K_v + BK) measured in accordance with the protocol shown on top, at pH_o 7.4 (black traces) and pH_o 6.6 (red traces). **b)** Pulse protocol used to determine the size of BK currents from total K⁺ currents. The blue trace with 500 μM Cd²⁺ is obtained with no pre-step depolarization to +20 mV and is used to determine the size of BK currents at pH_o 7.4 (black trace) and pH_o 7.0 (red trace) as indicated. **c)** Dependence of BK currents on pre-conditioning voltage at pH_o 7.4 (black dots) and pH_o 7.0 (red triangles). Notice the typical bell-shaped I/V curves expected for BK channels at both pH_o. The V_m of voltage-clamp recordings was not corrected for the LJPs (see Materials & Methods).

Fig. 7 - Lowering pH_o reduces markedly the size of BK currents at different voltages with little effect on the size of Kv and SK currents. **a)** BK currents measured in accordance with the protocol shown at pH_o 7.4 (black traces) and pH_o 7.0 (red traces), after subtracting the Kv currents remaining after 500 μM Cd²⁺ application. **b)** Current peak amplitudes were used to calculate the conductance (g_{BK}) versus voltage at pH_o 7.4, 7.0, 6.8 and 6.6, as indicated. g_{BK}(V) was calculated as described in Materials and Methods. Data were fit by a Boltzmann equation with V_{1/2} = 61.0 mV and k = 33.8 mV at pH_o 7.4, V_{1/2} = 49.9 mV and k = 28.4 mV at pH_o 7.0, V_{1/2} = 39.2 mV and k = 22.5 mV at pH_o 6.8, V_{1/2} = 36.9 mV and k = 21.0 mV at pH_o 6.6. **c)** pH_o dependence of BK currents normalized at pH_o 7.4, calculated from the maximal g_{BK} values at +120 mV. The continuous curve is a dose-response best fit with equation: % I_{BK} = % I_{BKmax} / 1 + 10^{-(IC₅₀ - pH) n} with % I_{BKmax} = 126, IC₅₀ = 7.0 and Hill slope n = 1.26. Data points are normalized to 7.4. **d)** Kv currents recordings at pH_o 7.4 (black trace) and pH 7.0 (red trace) at +90 mV in the presence of 300 nM TTX, 500 μM Cd²⁺, 1 μM paxilline and 200 nM apamin to block Nav, Cav, BK and SK channels. **e)** Current peak amplitudes were used to calculate the conductance (g_K) versus voltage at pH 7.4 (black squares) and 7.0 (red dots). **f)** SK tail currents elicited by the protocol shown on top at pH_o 7.4 (black trace) and pH_o 7.0 (red trace) and during addition of 200 nM apamin (blue trace). *Inset to the bottom:* Mean amplitude of SK tail currents at pH_o 7.4, pH_o 7.0 and with 200 nM apamin as indicated (n = 6 cells). Tail currents amplitude was estimated 20 ms after the onset of the hyperpolarization to -100 mV, when Kv channels are deactivated. The V_m of voltage-clamp recordings was not corrected for the LJPs (see Materials & Methods).

Fig. 8 - Mixtures of TASK-1 and BK channel blockers favor the switch from tonic to sustained burst firing in MCCs. *Bottom:* Representative current clamp trace of a spontaneously firing MCCs before and during bath application of 300 nM A1899 (TASK-1 blocker) alone and after addition of 300 nM paxilline (BK channel blocker). The black dotted line indicates the 0 mV level. White dashed lines indicate V_{rest} at control (pH_o 7.4) and with 300 nM A1899. *Top:* time expanded recordings corresponding to the grey windows indicated below. The switch from tonic (left panel) to intermittent

(center) and sustained burst firing (right) is evident. The V_m of current-clamp recordings was not corrected for the LJPs (see Materials & Methods).

Fig. 9 – Comparative analysis of burst firing parameters induced by low pH_o and TASK-1 plus BK channel blockers. *Top:* Examples of bursts recorded under the conditions indicated below, for $n = 10$ to 5 cells. The number of events in a burst, the 1st and last peak amplitude were derived directly from the data analysis software program. The mean plateau amplitude was estimated by calculating the half amplitude of the AHP that was assumed to increase linearly from the 1st to the last spike. Burst duration was calculated from the initial fast rising of the 1st AP to the end of the fast repolarization of the last AP, just before the onset of the slower repolarization phase. One-way ANOVA followed by Bonferroni post hoc tests were made by comparing the values at pH_o 6.6 (last column) with the values in each other condition (** $P < 0.01$). We considered $P < 0.01$ to be significantly different.

Fig. 10 – Increasing doses of nifedipine revert burst firing to tonic firing and then block. *Bottom:* Representative current clamp trace of a spontaneously firing MCCs before and during bath application of 300 nM A1899 + 300 nM paxilline (BK channel blocker). The cell displays an initial mild burst firing in control conditions (pH_o 7.4). Addition of saturating doses of the two blockers (300 nM A1899 + 300 nM paxilline) converts the firing in to sustained long lasting bursts of 0.3 to 1 s followed by profound hyperpolarizations (arrows in the top middle panel to the left). Addition of 300 nM nifedipine stops the bursts and subsequent addition of 3 μ M nifedipine causes a slight depolarization and blocks the firing. The black dotted line indicates the 0 mV level. White dashed lines indicate V_{rest} at control and with A1899 + paxilline. *Top:* Time expanded recordings, corresponding to the grey windows of different duration indicated below. The V_m of current-clamp recordings was not corrected for the LJPs (see Materials & Methods).

Fig. 11 – Nifedipine blocks burst firing evoked by brief step depolarizations. Three overlapped AP recordings induced by brief (100 ms) step depolarization of 20 pA from $V_h = -70$ in control

condition (pH_o 7.4; black trace), during pH_o 6.6 application (red trace) and during addition of 3 μM nifedipine to the pH_o 6.6 solution (blue trace). The dotted line indicates the 0 mV level. *Inset*: time expanded recording corresponding to the indicated grey window to the left. Nifedipine is effective in blocking the burst firing that persists after the cell is hyperpolarized to -70 mV while preserving the tonic firing during the brief depolarization. The V_m of current-clamp recordings was not corrected for the LJPs (see Materials & Methods).

Fig. 12 – **Effects of BayK8644 on spontaneous AP firing.** **a)** Representative current clamp trace of a spontaneously firing MCCs that switches from tonic to burst firing with increasing BayK8644 concentrations (0.1, 0.3 and 1 μM) applied sequentially. The time-expanded recordings (top grey windows) illustrate the increase in burst duration with increasing concentrations of BayK8644. **b)** Representative current clamp trace of a spontaneously firing MCC in which BayK8644 did not enhance burst firing. In this example, the DHP agonist increases only the rate of AP firing. Dotted lines indicate the 0 mV level. The V_m of current-clamp recordings was not corrected for the LJPs (see Materials & Methods).

Fig. 13 – **Burst firing induced by low pH_o and mixtures of A1899 + paxilline boosts MCCs exocytosis.** **a)** Example of simultaneous recordings of APs (bottom trace) and amperometric events (top trace) by carbon fibre amperometry at pH_o 7.4. **b)** Same recording conditions as in panel **a** with a perfusing solution of pH_o 6.6. **c)** Same recording conditions as in panel **a** and **b** in the presence of A1899 (300 nM) and paxilline (300 nM). To the right are shown the time expanded recordings of amperometric spikes and APs indicated to the left. **d)** Comparison of amperometric spikes parameters (see top representation), frequency and cubic root of cumulative charge (Q^{1/3}) between pH_o 7.4 (black bars), pH_o 6.6 (blue bars) and A1899 + paxilline (red bars) (* P < 0.05, ** P < 0.01 and *** P < 0.001, n = 8; one-way ANOVA followed by Bonferroni *post hoc* test). **e)** Overlap of cumulative secretion plots derived from amperometric measurements shown in **a**, **b** and **c** for control (pH_o 7.4; black trace), pH_o 6.6 (blue trace) and A1899 + paxilline (red trace). The V_m of current-clamp recordings was not corrected for the LJPs (see Materials & Methods).

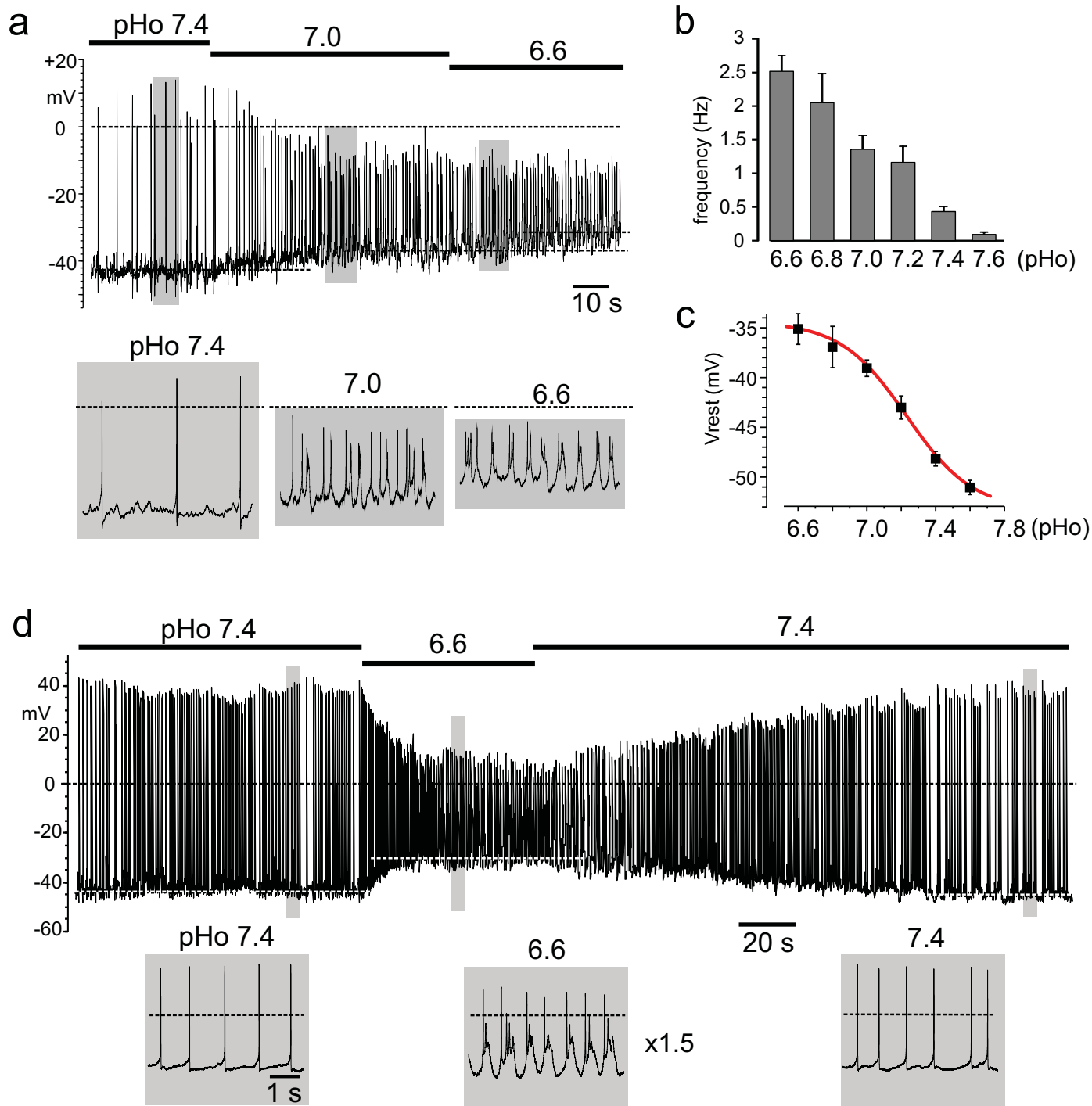


Fig.1

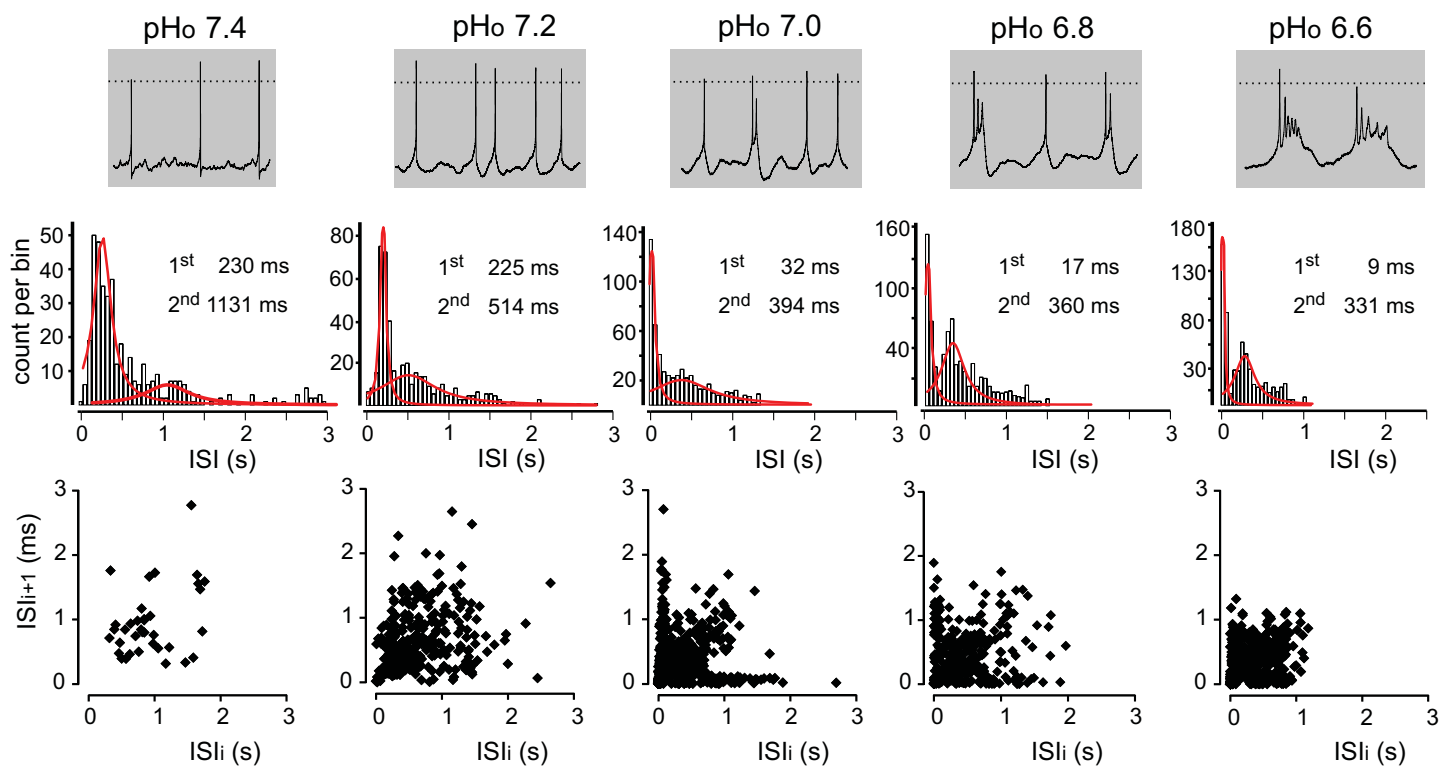


Fig.2

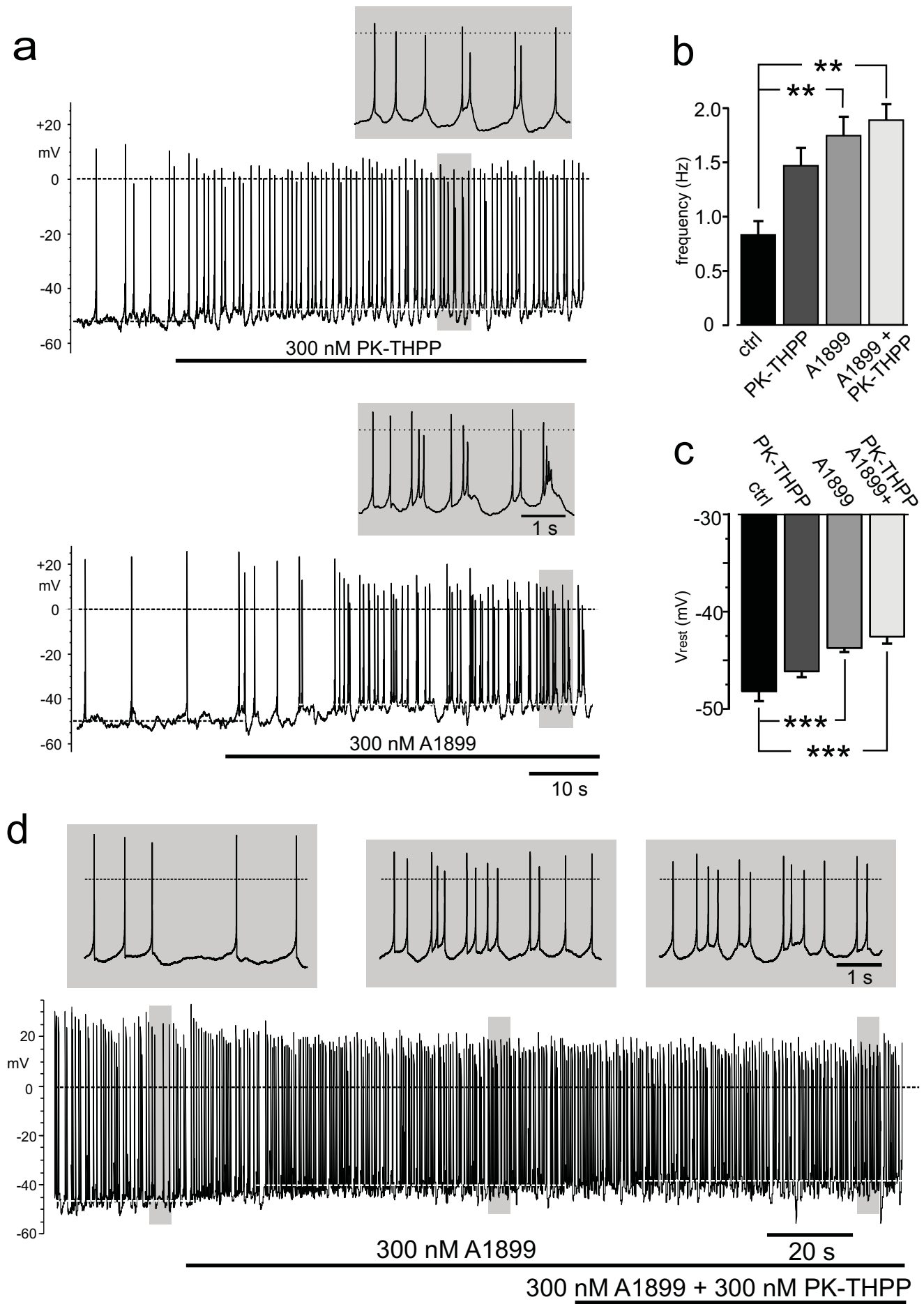


Fig.3

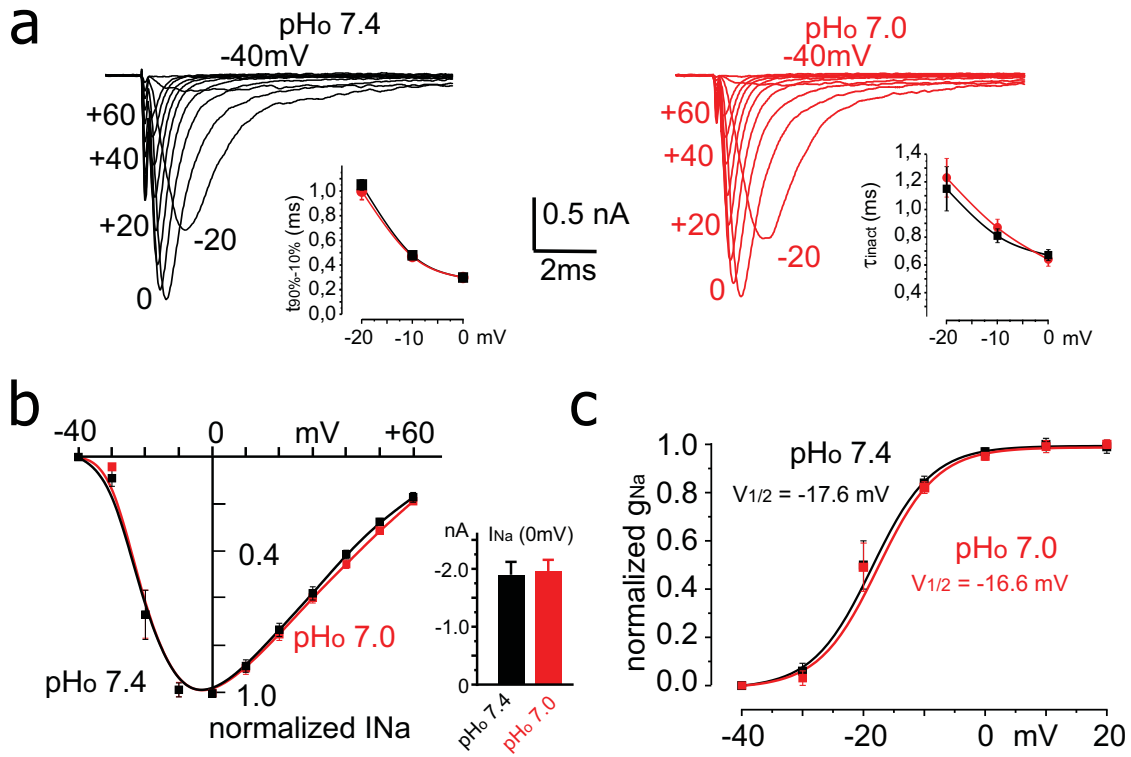


Fig.4

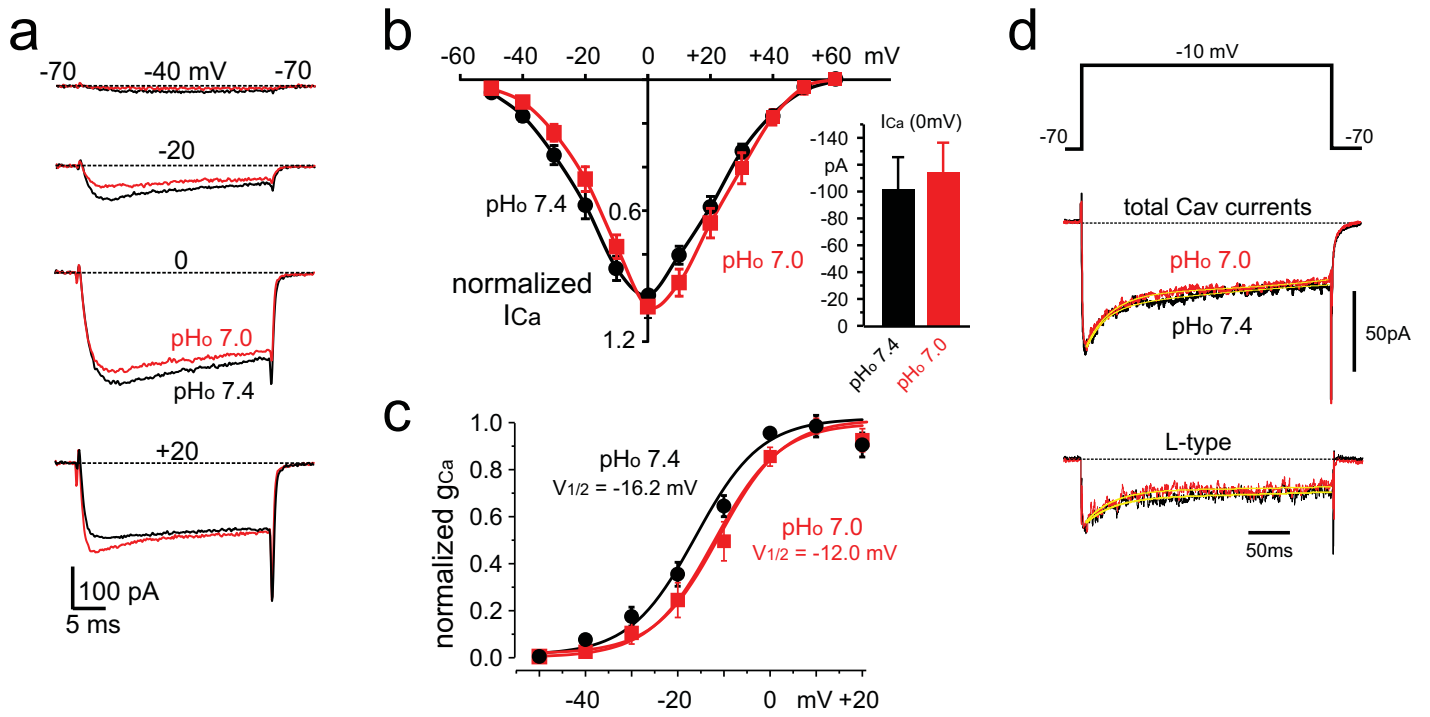


Fig.5

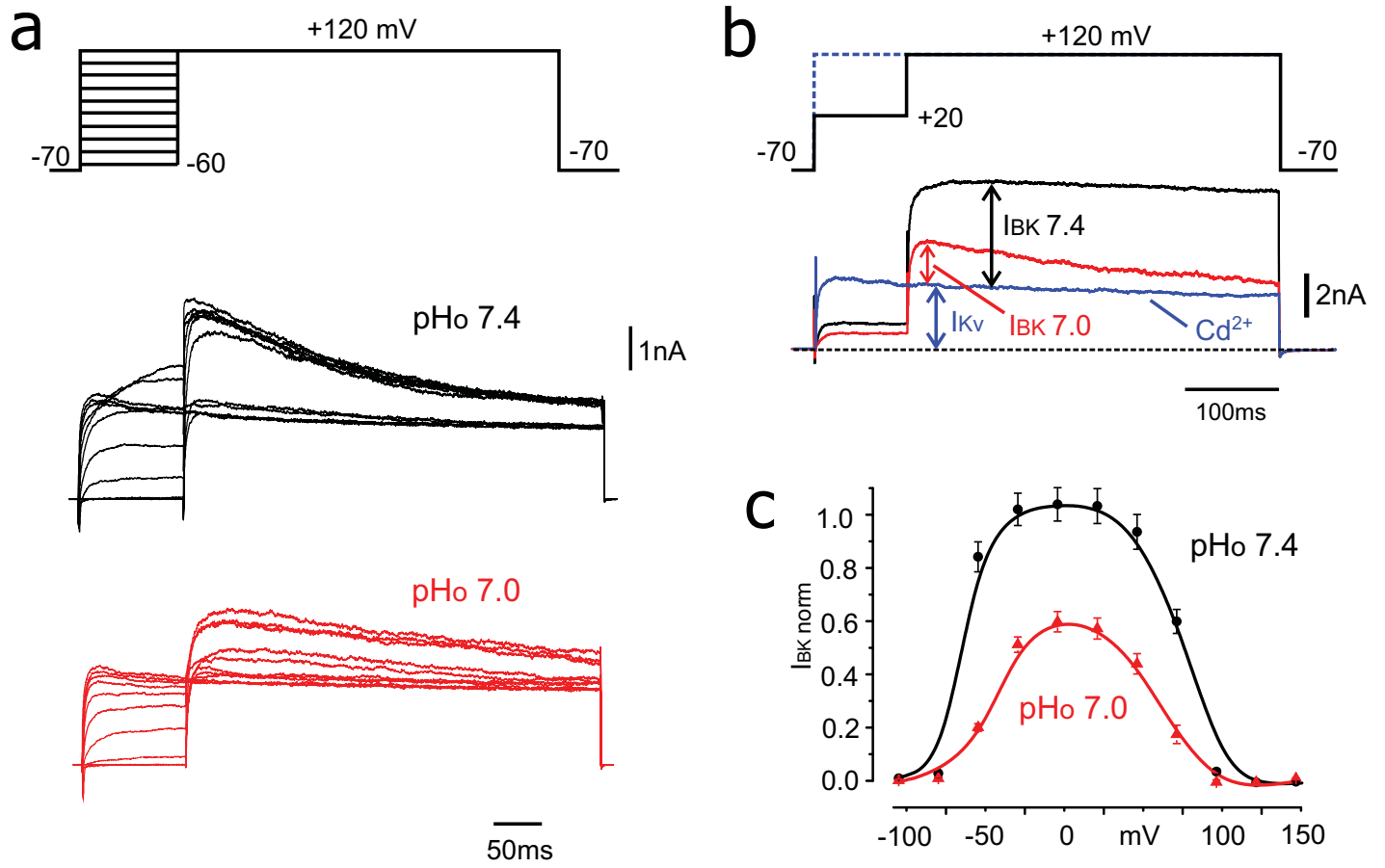


Fig.6

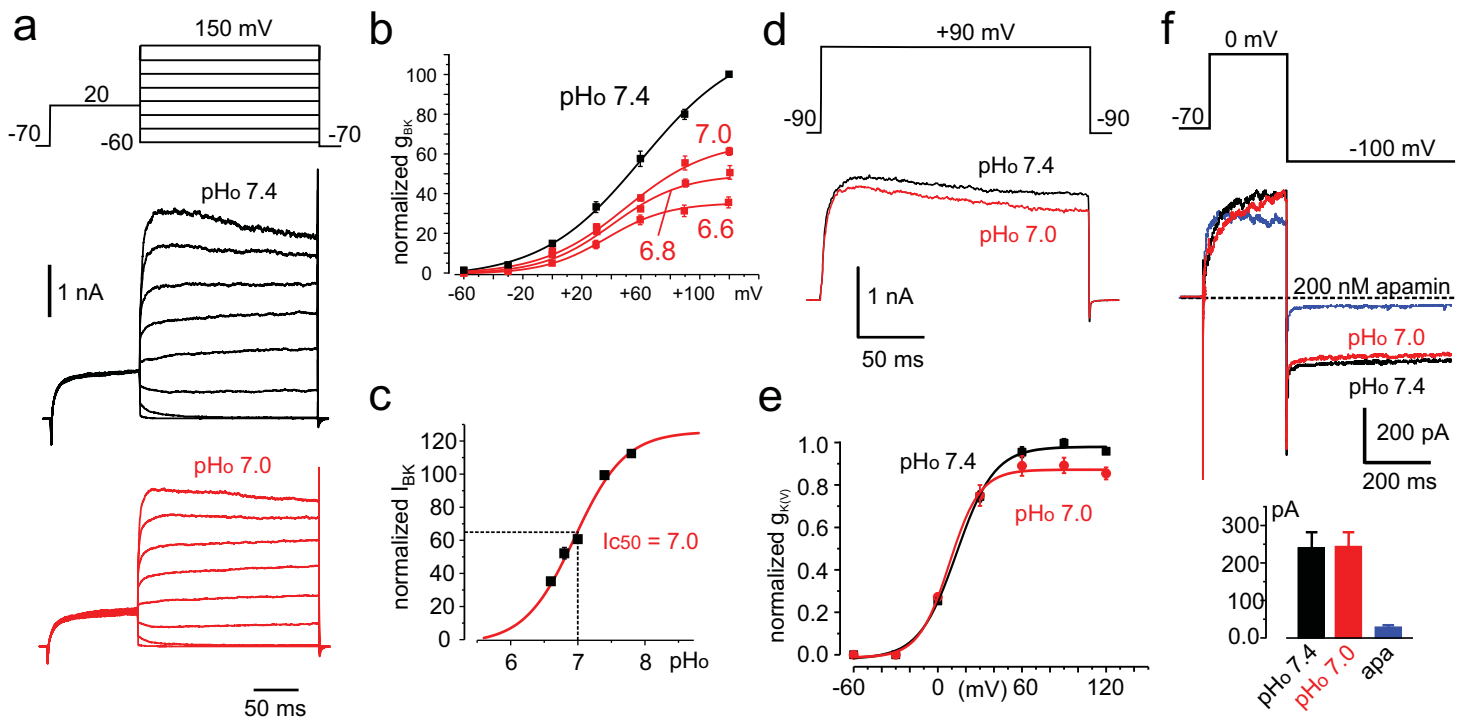


Fig.7

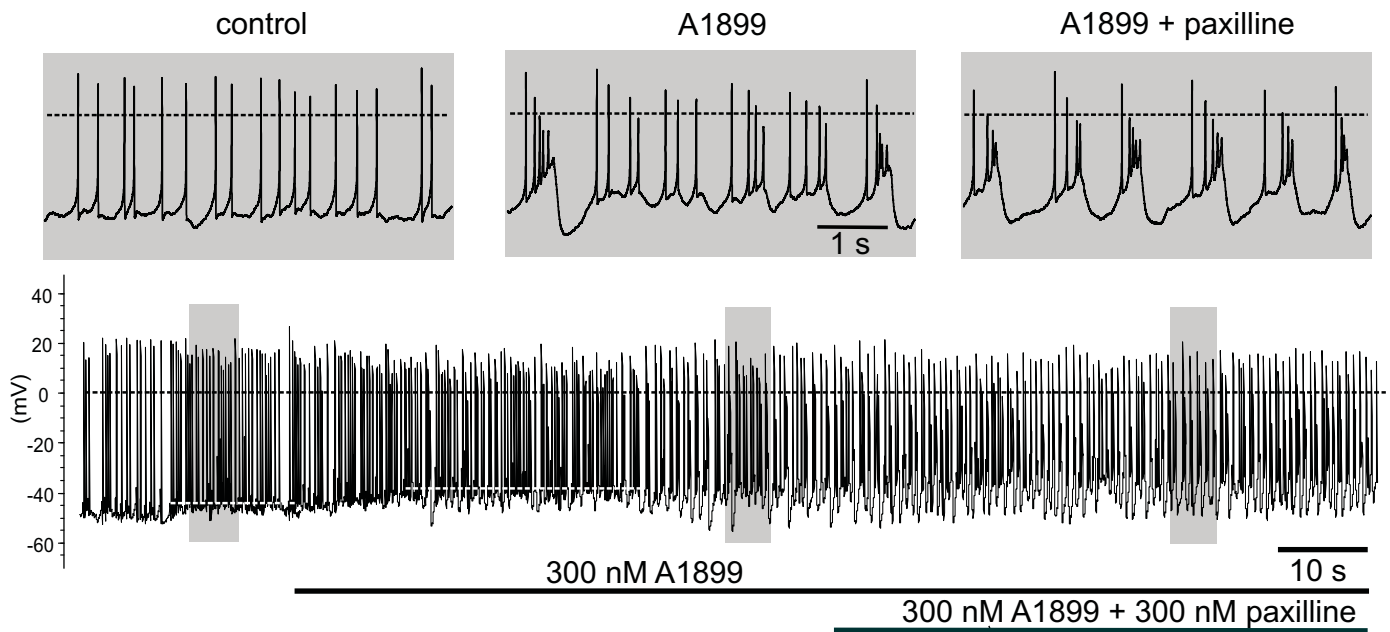
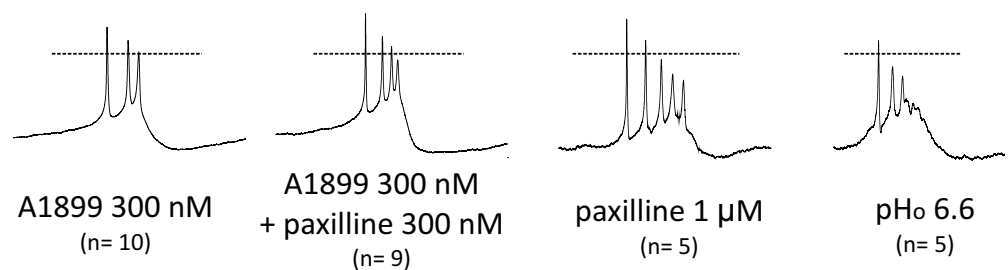


Fig.8



	A1899 300 nM (n= 10)	A1899 300 nM + paxilline 300 nM (n= 9)	paxilline 1 μM (n= 5)	pHo 6.6 (n= 5)
n° events in burst	3.6 ± 1.0	4.2 ± 1.3	4.8 ± 1.5	3.8 ± 1.3
burst duration (ms)	348.1 ± 21.7	314.7 ± 23.6	448.0 ± 19.0	328.0 ± 35.7
1st peak amplitude (mV)	8.8 ± 1.1	13.8 ± 1.0	12.3 ± 3.6	1.8 ± 2.1
last peak amplitude (mV)	-11.2 ± 1.6	-9.9 ± 1.5	-5.2 ± 3.0 **	-13.4 ± 1.9
mean plateau amplitude (mV)	-33.0 ± 0.4 **	-28.9 ± 0.7 **	-29.2 ± 0.7 **	-25.9 ± 0.9
n° bursts/min	12.0 ± 3.2 **	35.1 ± 7.6	25.5 ± 9.5	45.0 ± 3.8

Fig.9

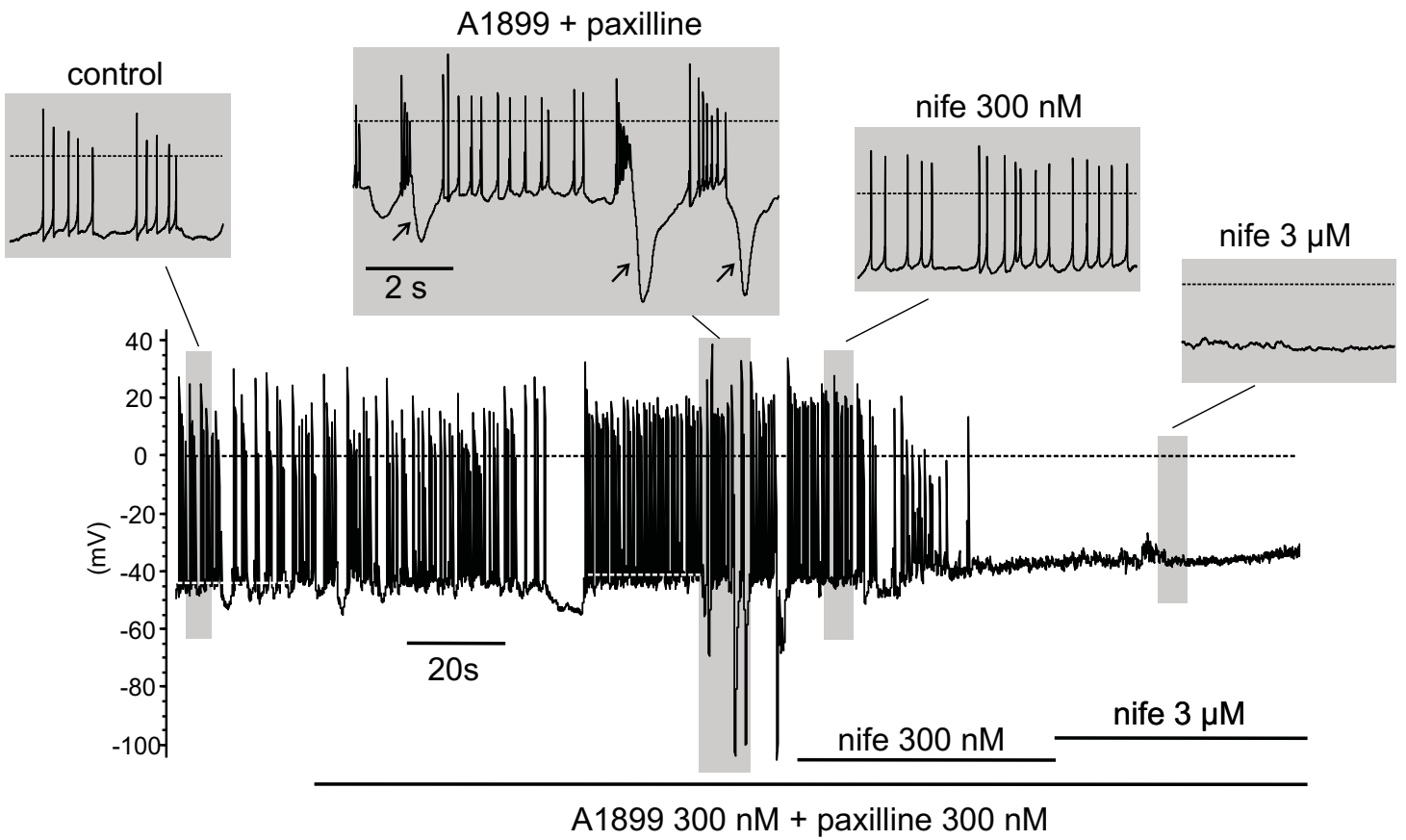


Fig.10

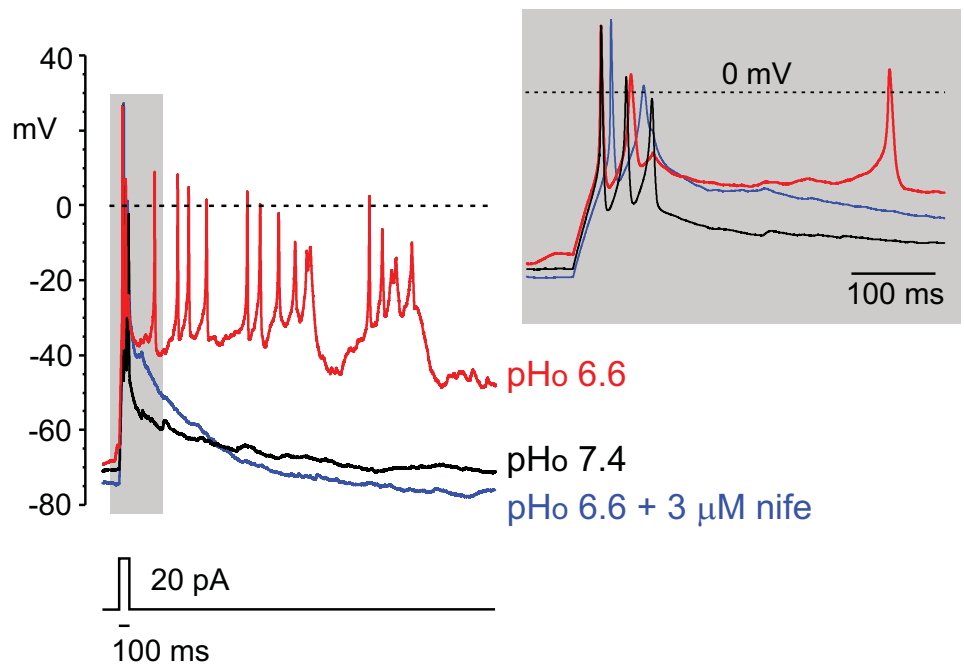


Fig.11

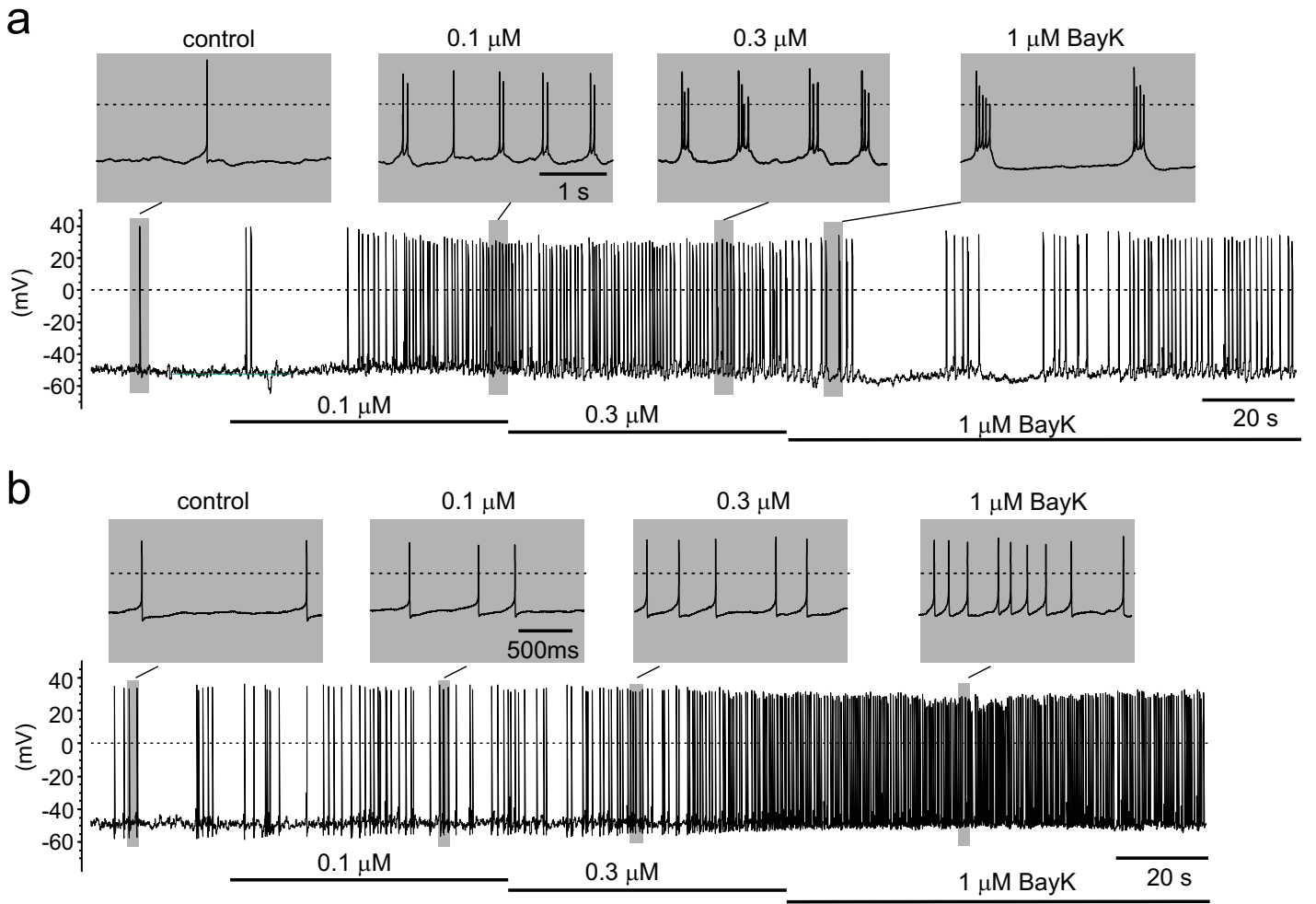


Fig.12

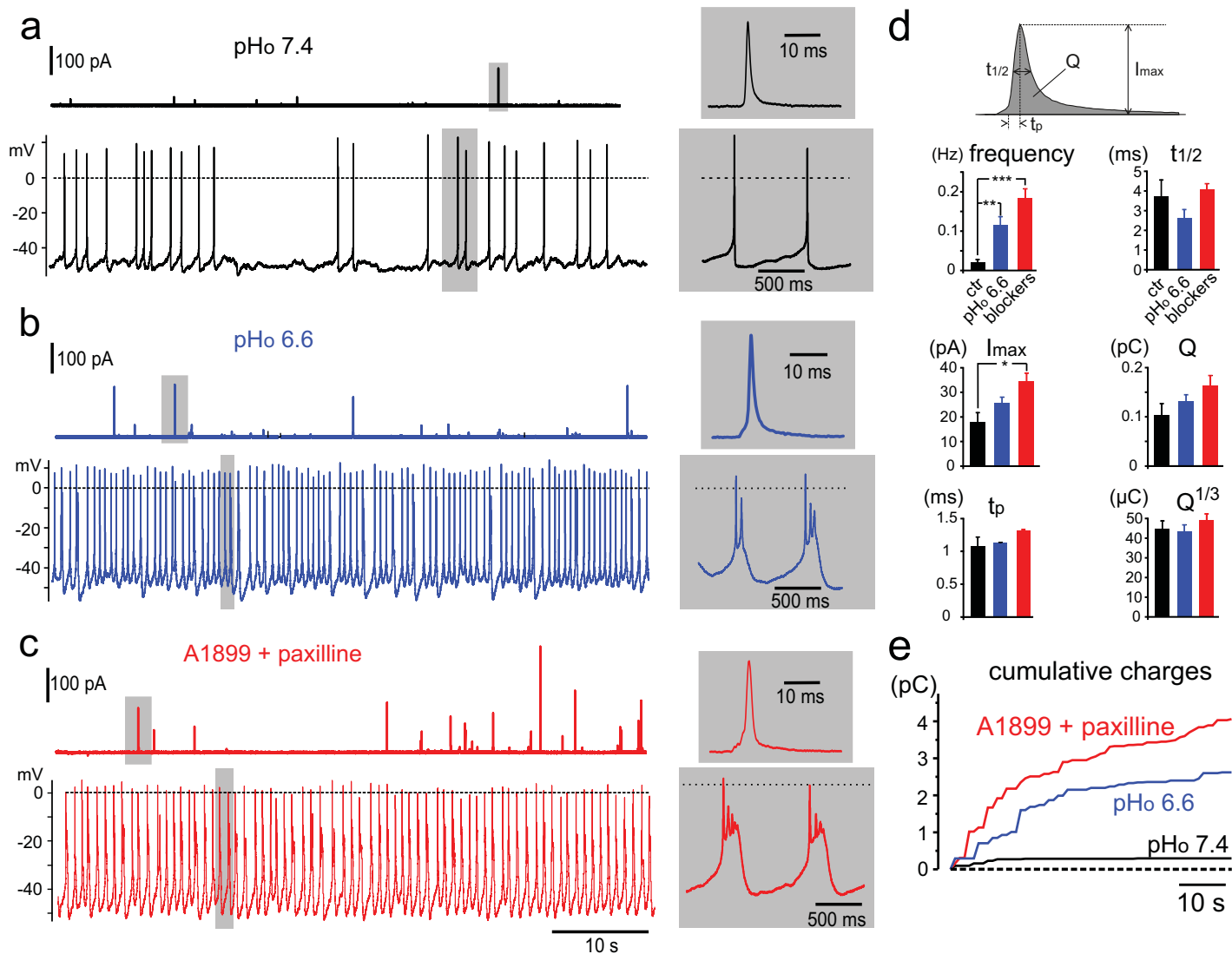


Fig.13